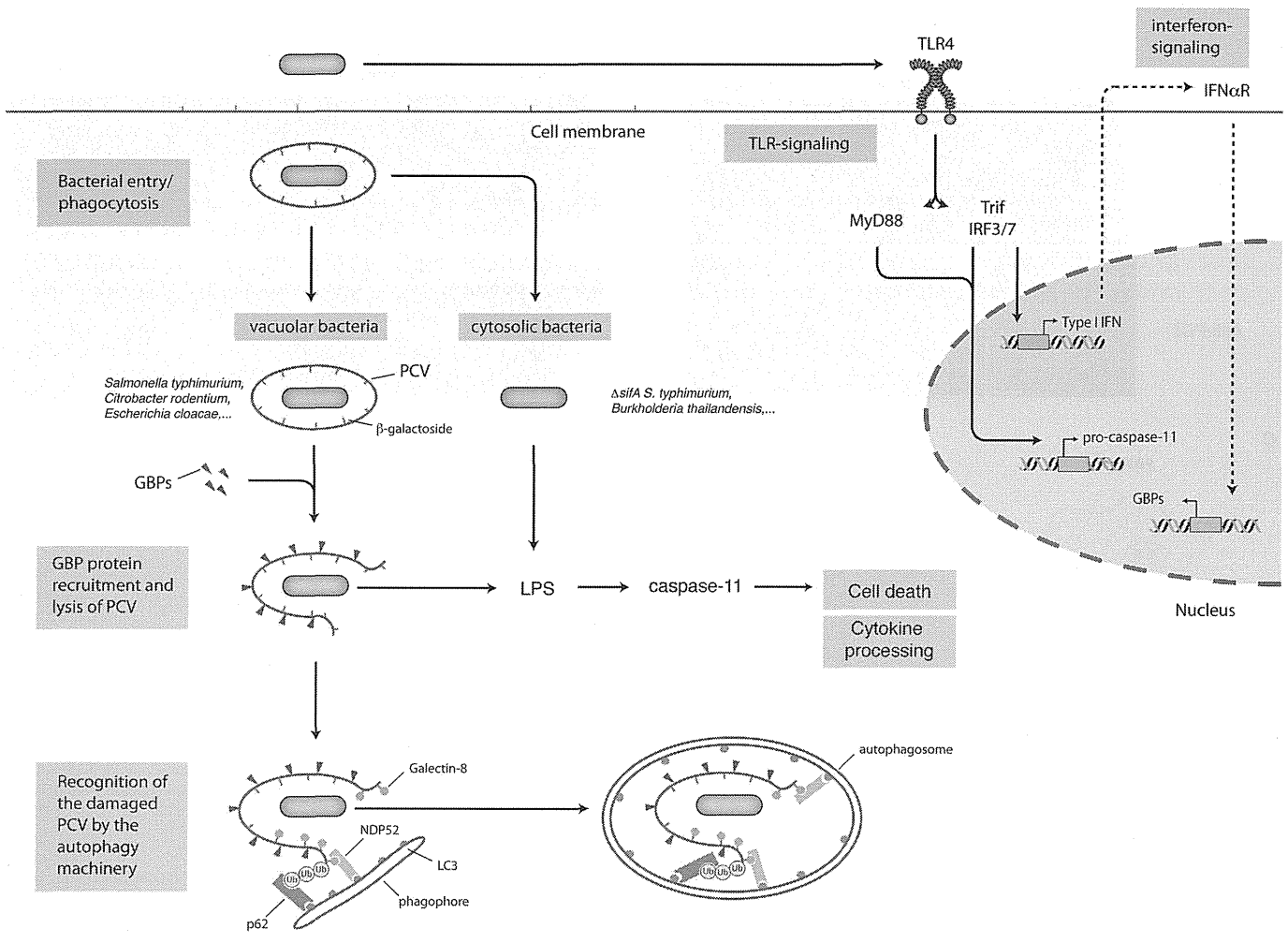

Extended Data Figure 10 | Model for the role of GBPs and autophagy in caspase-11 activation. The pathogen-containing vacuole of vacuolar bacterial pathogens is recognized by interferon-induced GBPs in an unknown manner. GBPs promote the lysis of the PCV either directly or indirectly, resulting in the release of the bacteria into the cytosol and activation of caspase-11 by bacterial LPS. β-galactosides of the lysed vacuole serve as danger signals upon exposure to the cytosol and are recognized by galectin-8 leading to the recruitment of the autophagy machinery. p62 participates in this process by recognizing ubiquitin-chains on the vacuole or the bacterium. Uptake of the bacterium and the lysed vacuole into autophagosomes reduces caspase-11 activation by removing the source of LPS from the cytosol.

CellPress

Immunity
Article

Foxp3$^+$ T Cells Regulate Immunoglobulin A Selection and Facilitate Diversification of Bacterial Species Responsible for Immune Homeostasis

Shimpei Kawamoto,[1,6] Mikako Maruya,[1,6] Lucia M. Kato,[1,6] Wataru Suda,[4] Koji Atarashi,[2] Yasuko Doi,[1] Yumi Tsutsui,[1] Hongyan Qin,[1,5] Kenya Honda,[2] Takaharu Okada,[3] Masahira Hattori,[4] and Sidonia Fagarasan[1,*]

[1]Laboratory for Mucosal Immunity
[2]Laboratory for Gut Homeostasis
[3]Laboratory for Tissue Dynamics
Center for Integrative Medical Sciences (IMS-RCAI), RIKEN Yokohama Institute, 1-7-22 Suehiro-cho, Tsurumi, Yokohama, 230-0045 Kanagawa, Japan
[4]Center for Omics and Bioinformatics, Graduate School of Frontier Sciences, The University of Tokyo, 5-1-5 Kashiwa-no-ha, Kashiwa, 277-8561 Chiba, Japan
[5]Department of Medical Genetics and Developmental Biology, 4th Military Medical University, Chang-Le Xi Street #17, Xi'an 710032, China
[6]Co-first author
*Correspondence: sidonia-f@rcai.riken.jp
http://dx.doi.org/10.1016/j.immuni.2014.05.016

SUMMARY

Foxp3$^+$ T cells play a critical role for the maintenance of immune tolerance. Here we show that in mice, Foxp3$^+$ T cells contributed to diversification of gut microbiota, particularly of species belonging to Firmicutes. The control of indigenous bacteria by Foxp3$^+$ T cells involved regulatory functions both outside and inside germinal centers (GCs), consisting of suppression of inflammation and regulation of immunoglobulin A (IgA) selection in Peyer's patches, respectively. Diversified and selected IgAs contributed to maintenance of diversified and balanced microbiota, which in turn facilitated the expansion of Foxp3$^+$ T cells, induction of GCs, and IgA responses in the gut through a symbiotic regulatory loop. Thus, the adaptive immune system, through cellular and molecular components that are required for immune tolerance and through the diversification as well as selection of antibody repertoire, mediates host-microbial symbiosis by controlling the richness and balance of bacterial communities required for homeostasis.

INTRODUCTION

The main function of the immune system is to protect the host against pathogens, such as bacteria or viruses. However, unlike the systemic immune system, the gut immune system does not eliminate microorganisms but instead nourishes rich bacterial communities and establishes advanced symbiotic relationships (Sutherland and Fagarasan, 2012). Not only are the gut bacteria essential for nutrient processing, production of vitamins, and protection against pathogens (through competition for space and nutrients), but the development and maturation of the immune system depends on these bacteria (Fagarasan et al., 2010; Geuking et al., 2011; Hooper et al., 2012; Sutherland and Fagarasan, 2012). The primary individual microbiota (Mb) composition probably reflects the maternal hand-over during or immediately after birth (Kau et al., 2011; Nicholson et al., 2012). However, the subsequent shaping of the microbial landscape is probably driven by complex interactions with the host immune system, through a network of regulatory components involving both the innate and adaptive immune system (Fagarasan et al., 2010; Hooper et al., 2012; Maynard et al., 2012).

Our previous studies demonstrated that the absence of immunoglobulin A (IgA) (the major effector molecule of the adaptive immunity in the gut) or the impaired IgA selection in germinal centers (GCs) due to deregulated T cell control severely affects the balance of gut bacterial communities, resulting in massive activation of the whole body immune system (Fagarasan et al., 2002; Kawamoto et al., 2012; Suzuki et al., 2004; Wei et al., 2011). The absence of a subset of Foxp3$^+$ T cells induced by bacterial antigens also modifies the composition of gut Mb by evoking mucosal T helper 2 (Th2) cell-mediated inflammation (Josefowicz et al., 2012). Interestingly, the Foxp3$^+$ T cells induce GC and IgA responses by generating GC T cells (Tsuji et al., 2009), and their depletion causes a rapid loss of specific IgA responses in the intestine (Cong et al., 2009). Together, all these observations point to the existence of a Foxp3-IgA axis in maintaining the balance of gut Mb. It remains unclear, however, how these specific arms of the adaptive immune system mediate host-microbial interactions in the gut.

We show that Foxp3$^+$ T cells, by acting in both GC-independent and -dependent manners, repress inflammation and support IgA selection in the GCs of Peyer's patches (PPs), resulting in diversification of gut Mb. Balanced and diverse Mb stimulates, in turn, the host immune system by promoting the expansion of Foxp3$^+$ T cells and induction of GC and IgA production in the gut through a symbiotic regulatory loop.

RESULTS

Reduced Diversity of Gut Microbiota in Immunodeficient Mice

We evaluated the impact of acquired immunity on gut Mb by analyzing various mice that partially or completely lack cellular and structural components of the adaptive immune system in gut. We found that mice lacking both B and T cells (*Rag1*$^{-/-}$), and as such having just rudimentary PPs, have considerably less diverse bacterial communities compared with *Rag1*$^{+/-}$ littermates or with wild-type (WT) mice raised in the same facility (Figure S1A available online). Not only the *Rag1*$^{-/-}$ mice, but also mice lacking only B cells (*Ighm*$^{-/-}$) or T cells (*Cd3e*$^{-/-}$), and thus lacking GCs, also had reduced bacterial diversity and different phylogenetic structures of bacterial communities compared with their heterozygous littermates or WT mice (Figures S1A and S1B). The results indicate that the adaptive immune system and its functionally organized follicular structures (i.e., PPs with GCs) facilitated diversification and influenced the structures of bacterial communities in gut.

Foxp3$^+$ T Cells Are Required for Maintenance of Diverse Microbial Communities in Gut

Given that the PPs are enriched in B cells that interact mainly with CD4$^+$ T cells, we next asked which CD4$^+$ T cell subset(s) contribute to diversity and composition of gut Mb. For this, we transferred distinct CD4$^+$ T cell populations (naive CD4$^+$ T cells and Foxp3$^+$ T cells) into *Cd3e*$^{-/-}$ mice, and the Mb were assessed 10–12 weeks after the injection. The transfer of naive CD4$^+$ T cells alone (isolated from the spleen and peripheral lymph nodes of WT mice) considerably decreased bacterial diversity even below that observed in *Cd3e*$^{-/-}$ mice (Figure 1A). The change was associated with gut inflammation caused by expansion of T cells with inflammatory properties (Figures 2A, 2B, and 2E). Therefore, in mice, similar to humans, the inflammatory environment due to deregulated T cell populations did not afford the maintenance of complex bacterial communities (Manichanh et al., 2006; Nishikawa et al., 2009; Ott et al., 2004). Furthermore, the transfer of naive CD4$^+$ T cells failed to increase bacterial diversity even in the absence of overt inflammation (i.e., in mice treated with anti-IL-12p40 that had considerably reduced expansion of inflammatory T cells and no signs of wasting disease or colitis) (Figures S1C–S1G). The cotransfer of naive CD4$^+$ T cells along with Foxp3$^+$ T cells led to reconstitution of the microbial diversity to levels observed in WT mice (Figure 1A). Not only the diversity but also the phylogenetic structures of bacterial communities become more similar to WT mice when naive CD4$^+$ T cells were transferred together with Foxp3$^+$ T cells (Figure 1B). In fact, the transfer of Foxp3$^+$ T cells alone increased bacterial diversity and modified the composition of Mb in *Cd3e*$^{-/-}$ mice almost to the degree found in WT mice (Figures 1A and 1B). Strikingly, the Foxp3$^+$ T cells facilitated the diversification of Firmicutes, particularly of nonpathogenic Clostridia belonging to cluster IV and XIVa, which were recently reported to be effective inducers of Foxp3$^+$ T cells in the gut (Figure 1C; Atarashi et al., 2011, 2013). Thus, not only can Firmicutes induce Foxp3 expression, but Foxp3$^+$ T cells can in turn feedback to Mb facilitating the maintenance and diversification of these major spore-forming bacteria. Taken together, the presence of Foxp3$^+$ T cells was required for the establishment of complex bacterial communities in both inflammatory and noninflammatory environments in the gut.

Requirement for Foxp3$^+$ T Cells Acting as Tfr Cells for Gut Microbiota Regulation

Foxp3$^+$ T cells could exert their regulatory effect on Mb in multiple ways. They could do it simply by preventing the expansion of Foxp3$^-$ T cells and their excessive production of cytokines and therefore by controlling inflammation in a GC-independent manner (Izcue et al., 2006; Josefowicz et al., 2012). Alternatively, the Foxp3$^+$ T cells could act through their regulatory roles on PP GCs and IgA synthesis, by becoming T follicular regulatory (Tfr) (CXCR5^{hi}PD1^{hi}Foxp3$^+$) and T follicular helper (Tfh) (CXCR5^{hi}PD1^{hi}Foxp3$^-$) cells, as previously reported (Chung et al., 2011; Cong et al., 2009; Linterman et al., 2011; Tsuji et al., 2009; Wollenberg et al., 2011). The transfer of Foxp3$^+$ T cells into *Cd3e*$^{-/-}$*Aicda*$^{-/-}$ mice (which lack both T cells and antibodies others than IgM), failed to increase Mb diversity even though the cells expanded well and generated considerably more GCs, including Tfh and Tfr cells in PPs (Figures 1D and 1E). This observation strongly suggests that the Foxp3$^+$ T cells contributed to shape the Mb and supported the gut mutualism by regulation of IgA production in the intestine.

The generation of both Tfr and Tfh cells depends on activation and induction of Bcl6 expression (Chung et al., 2011; Johnston et al., 2009; Linterman et al., 2011; Nurieva et al., 2009; Yu et al., 2009). To discriminate between the regulatory functions outside and inside the GCs, we performed experiments with Foxp3$^+$ T cells sufficient or deficient for Bcl6 expression isolated from WT mice and *Bcl6*$^{yfp/yfp}$ mice, respectively, in which the function of Bcl6 was inactivated by yellow fluorescent protein (YFP) insertion (Kitano et al., 2011). Thus, naive CD4$^+$ T cells were cotransferred at a 1:1 ratio with CD4$^+$CD25$^+$ T cells (more than 98% of which expressed Foxp3) from WT mice (hereafter CD25$^+$WT T cells) or from *Bcl6*$^{yfp/yfp}$ mice (hereafter CD25$^+$ *Bcl6*$^{yfp/yfp}$ T cells) into *Cd3e*$^{-/-}$ mice. In the presence of naive CD4$^+$ T cells, both CD25$^+$ WT T cells and CD25$^+$*Bcl6*$^{yfp/yfp}$ T cells had a similar expansion and maintenance of Foxp3 expression (Figure S2A). Furthermore, both CD25$^+$ WT T cells and CD25$^+$*Bcl6*$^{yfp/yfp}$ T cells prevented the expansion of naive T cells in the gut and there were no signs of mucosal inflammation or wasting disease in these transferred mice (Figures 2A–2D). Accordingly, the production of cytokines like IFN-γ and TNF-α was reduced whereas that of IL-10 was increased in the presence Foxp3$^+$ T cells, regardless of their Bcl6 expression (Figure 2E). Both groups of mice remained protected from inflammation even 6 months after the transfer (Figures S3A–S3C). Therefore, in the gut, Foxp3$^+$ T cells controlled the expansion of naive CD4$^+$ T cells and their production of proinflammatory cytokines, independently of Bcl6 expression. However, CD25$^+$*Bcl6*$^{yfp/yfp}$ T cells failed to normalize the bacterial diversity, which remained considerably lower than that observed in the presence of CD25$^+$ WT T cells (Figure 2F). The phylogenetic structures of bacterial communities in mice transferred with naive CD4$^+$ T cells together with CD25$^+$*Bcl6*$^{yfp/yfp}$ T cells, although distinct from mice transferred with naive CD4$^+$ T cells alone, remained different from those in mice cotransferred with

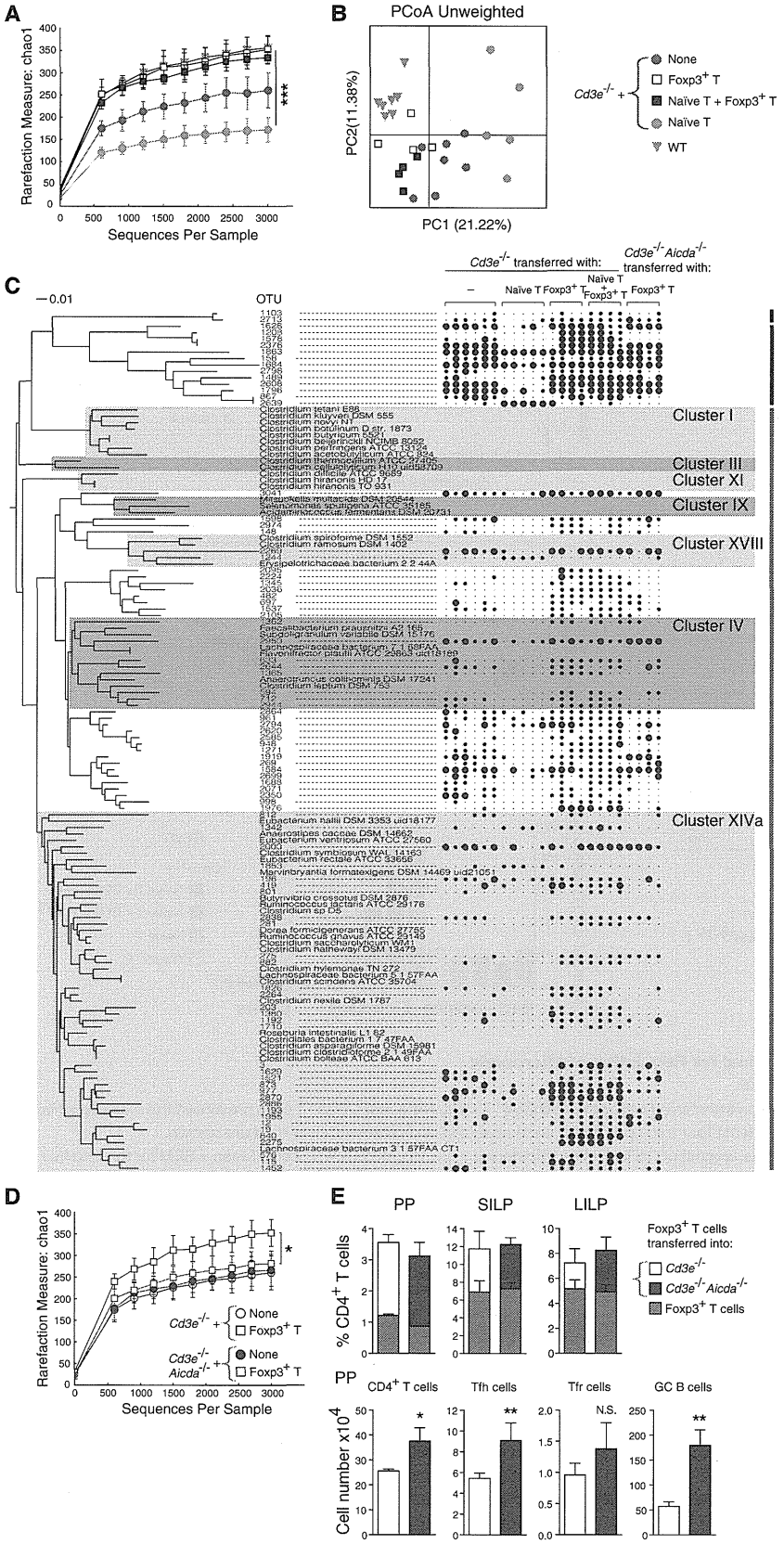

Figure 1. Increased Diversity of Firmicutes by Foxp3$^+$ T Cells

(A and D) Diversity of bacterial species (>97% identity) as indicated by Chao1 rarefaction measure based on 1–3,000 sequences.

(B) Unweighted UniFrac plot, comparing phylogenetic differences between microbial communities, clustered by principal coordinate analysis (PCoA).

(C) Phylogenetic analysis of OTUs associated with the presence of Foxp3$^+$ T cells. OTUs were defined and quantified by QIIME, followed by t test analyses between the Foxp3-deficient group (naive CD4$^+$ T cells transferred mice) and the Foxp3-sufficient group (Foxp3$^+$ T cells transferred alone or along with naive CD4$^+$ T cells). OTUs with statistically significant difference ($p < 0.05$) are shown. The results of nontransferred *Cd3e*$^{-/-}$ or *Cd3e*$^{-/-}$*Aicda*$^{-/-}$ mice transferred with Foxp3$^+$ cells are shown in parallel. The 16S rRNA sequences of statistically different OTUs ($p < 0.05$) were used to construct the phylogenetic tree. The sequences of other Clostridia bacteria used for the tree were obtained from known genome sequences or ribosomal database project. The calculation was performed with the MEGA v.5.1 package and the neighbor-joining method with a bootstrap of 500 replicates. Circle size correlates with the relative abundance of each OTU. Large circles, medium circles, and small dots indicate ≥1%, <1%, and 0%, respectively.

(E) The percentage of CD4$^+$ T cells in the gut and the numbers of indicated cell populations in *Cd3e*$^{-/-}$ and *Cd3e*$^{-/-}$*Aicda*$^{-/-}$ mice transferred with Foxp3$^+$ cells.

Mean ± SEM for four to seven mice per group. Two-tailed unpaired Student's t test was used to compare between (A) WT and *Cd3e*$^{-/-}$ + naive CD4$^+$ T cells and between (D and E) *Cd3e*$^{-/-}$ and *Cd3e*$^{-/-}$*Aicda*$^{-/-}$ mice transferred with Foxp3$^+$ cells; ***$p < 0.001$, **$p < 0.01$, *$p < 0.05$, N.S., no significant difference. See also Figure S1.

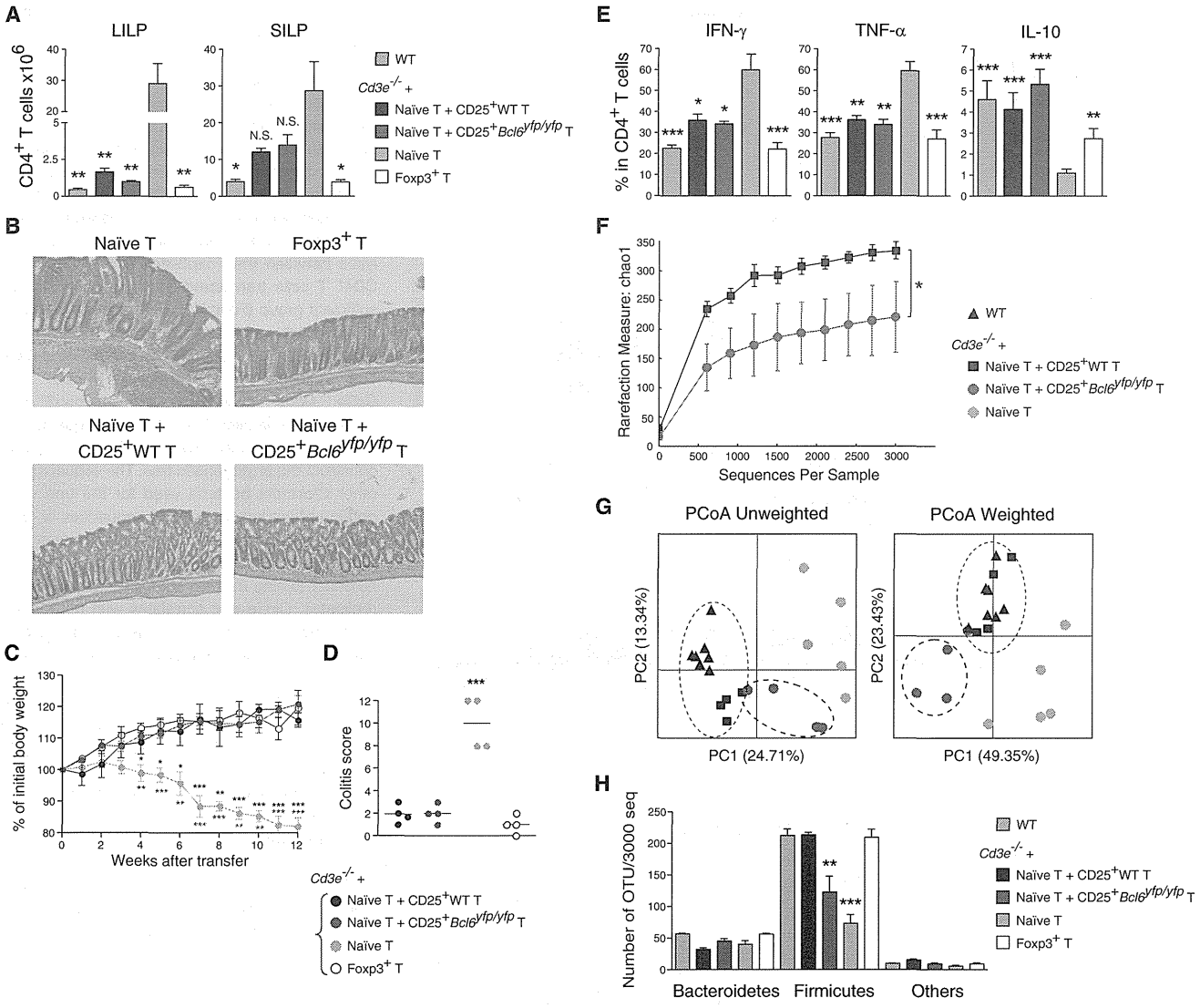

Figure 2. Foxp3$^+$ T Cell Migration into PP GCs Is Critical for Regulation of Microbiota

(A) Total numbers of CD4$^+$ T cells isolated from LILP and SILP.

(B) Hematoxylin-eosin staining sections of LI from *Cd3e*$^{-/-}$ mice transferred with indicated CD4$^+$ T cells. Note that CD25$^+$ T cells prevented the massive infiltration of inflammatory cells regardless of their Bcl6 expression. At least four mice per group were analyzed and representative data are shown.

(C) The change of body weight (presented as percent of original weight) of *Cd3e*$^{-/-}$ mice transferred with indicated CD4$^+$ T cells. Mean ± SEM for three to five mice per group.

(D) Colitis score for *Cd3e*$^{-/-}$ mice transferred with indicated T cells. Each point represents an individual mouse.

(E) Frequency of IFN-γ^+, TNF-α^+, and IL-10$^+$CD4$^+$ T cells from SILP of *Cd3e*$^{-/-}$ mice transferred with the indicated CD4$^+$ T cell subsets or from WT mice. Means ± SEM for four to six mice per group.

(F) Diversity of bacterial species as indicated by Chao1 rarefaction measure based on 1–3,000 sequences in *Cd3e*$^{-/-}$ mice transferred with indicated CD4$^+$ T cell subsets; four mice per group were analyzed.

(G) Communities clustered by principal coordinates analyses of the unweighted and weighted UniFrac distances (which measure qualitative and quantitative differences between microbial communities, respectively).

(H) Species diversity (numbers of OTUs/3,000 sequences) in cecal contents from WT or *Cd3e*$^{-/-}$ mice 10–12 weeks after the transfer of indicated CD4$^+$ T cell subsets. Mean ± SEM from four to seven mice per group.

Two-tailed unpaired Student's t test was used to compare between the indicated mouse groups and (A and E) *Cd3e*$^{-/-}$ mice transferred with naive CD4$^+$ T cells, (C) *Cd3e*$^{-/-}$ mice transferred with naive T cells along with CD25$^+$ WT T cells or CD25$^+$*Bcl6*$^{yfp/yfp}$ T cells, (D) other transferred mouse groups, (F) *Cd3e*$^{-/-}$ mice transferred with naive CD4$^+$ T cells together with CD25$^+$ WT T cells, or (H) WT mice; ***$p < 0.001$; **$p < 0.01$; *$p < 0.05$; N.S., no significant difference. See also Figure S2.

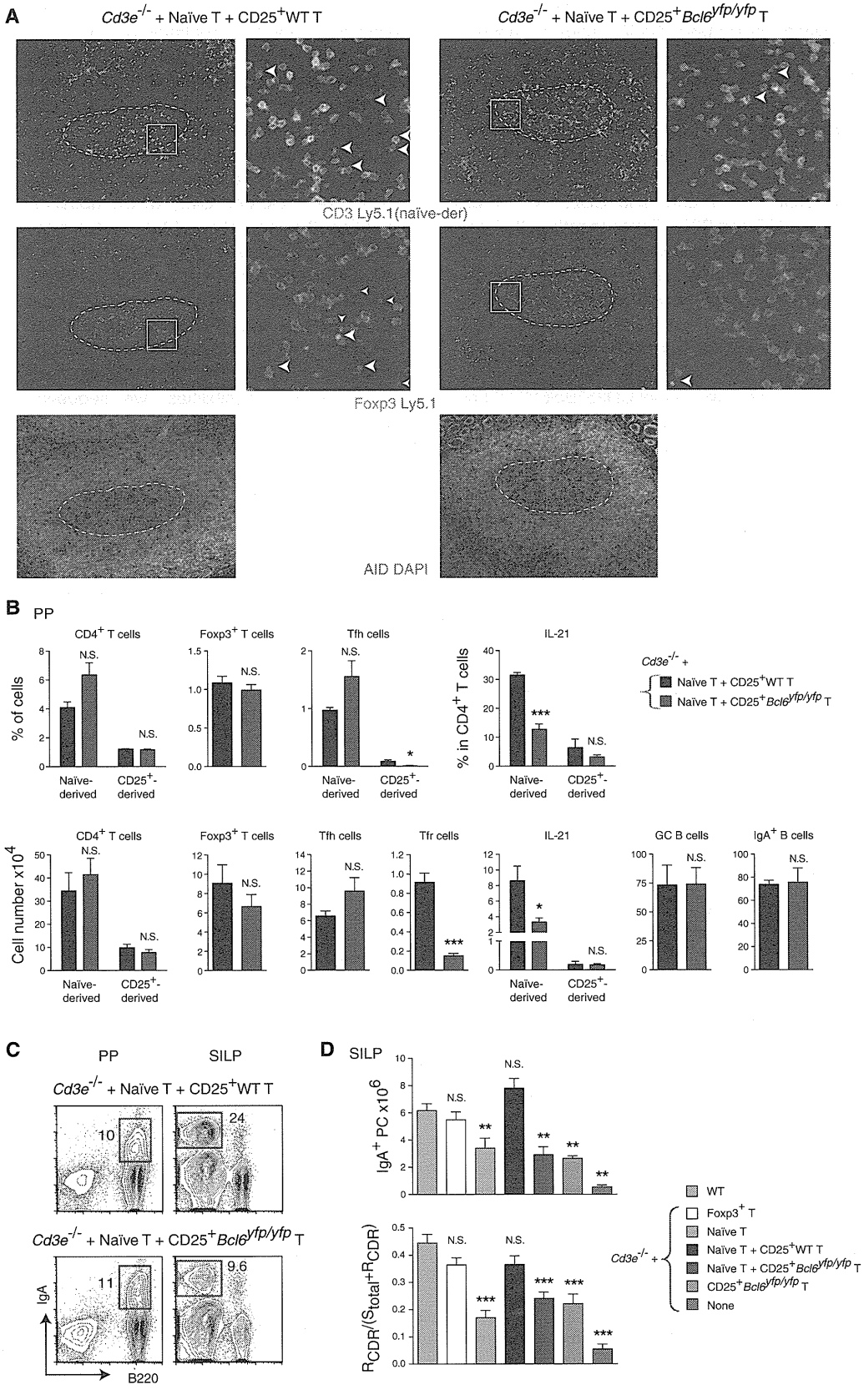

(legend on next page)

CD25$^+$ WT T cells (Figure 2G). Thus, we observed a pronounced reduction in diversity of Firmicutes in *Cd3e*$^{-/-}$ mice cotransferred with CD25$^+$*Bcl6*$^{yfp/yfp}$ T cells compared with mice cotransferred with CD25$^+$ WT T cells or WT mice (Figure 2H). The decrease in Firmicutes diversity was mostly due to the excessive expansion of species belonging to *Lachnospiraceae*, which induced an overall shift in bacterial communities with an increase in the ratio of Firmicutes to Bacteroidetes (2.05 and 0.73 in mice cotransferred with CD25$^+$*Bcl6*$^{yfp/yfp}$ T cells and CD25$^+$ WT T cells, respectively) (Figures S2B and S2C). Taken together, the results indicate that the maturation and differentiation of Foxp3$^+$ T cells into GC Tfr or Tfh cells, which depends on Bcl6 expression, was important for maintaining symbiosis with gut Mb.

Foxp3$^+$ T Cells Regulate Both Quantities and Qualities of IgAs

The cotransfer of naive T cells with either CD25$^+$*Bcl6*$^{yfp/yfp}$ T cells or CD25$^+$ WT T cells equally induced GCs in PPs, but with very different features (Figure 3A). Thus, the mice that received naive CD4$^+$ T cells and CD25$^+$*Bcl6*$^{yfp/yfp}$ T cells almost completely lacked Tfr cells yet contained many Tfh cells mostly derived from the naive CD4$^+$ T cells (Figures 3A and 3B). In contrast, the mice that received naive CD4$^+$ T cells with CD25$^+$ WT T cells had GCs with apparently more Tfr cells and fewer Tfh cells (some of them also generated from CD25$^+$ WT T cells upon downregulation of their Foxp3 expression) (Figures 3A, top and middle, and 3B). Interestingly, the production of IL-21 by PP T cells was considerably reduced in mice cotransferred with CD25$^+$*Bcl6*$^{yfp/yfp}$ T cells, suggesting that the presence of Foxp3$^+$ T cells in GCs might regulate cytokine production by Tfh cells (Figure 3B).

Strikingly, although there were no obvious differences in IgA$^+$ B cells in PPs (Figures 3B and 3C), the frequencies and numbers of IgA plasma cells in the small intestine lamina propria (SILP) were much decreased in mice cotransferred with CD25$^+$*Bcl6*$^{yfp/yfp}$ T cells (Figures 3C and 3D). More importantly, the IgAs produced in the absence of Bcl6 expression by Foxp3$^+$ T cells had a decreased affinity maturation index, suggesting defective selection in the GCs, in agreement with previous observations (Figure 3D; Linterman et al., 2011). In contrast, the CD25$^+$ WT T cells cotransferred with naive CD4$^+$ T cells reconstituted the SILP of *Cd3e*$^{-/-}$ mice with high numbers of apparently well-selected IgA plasma cells (Figures 3C and 3D). Thus, Foxp3$^+$ T cell presence in the GCs was critical for regulating both the qualities and frequencies of IgAs in the gut.

Quality of IgAs Regulates Diversity of Microbiota

Because GC and IgA regulation by Foxp3$^+$ T cells appeared to contribute considerably to shaping of gut Mb, we next evaluated the bacteria-coating properties of IgAs elicited in the presence or absence of Foxp3$^+$ T cells. Therefore, we stained fecal bacteria-bound IgA with antibodies recognizing both IgA heavy (V_H) and light (V_K) chains and established a setting and acquisition mode that allowed a clear separation of IgA-coated bacteria (Figures 4A, S4A, and S4B). In the absence of Foxp3$^+$ T cell regulation, the proportion of IgA-coated bacteria increased, as did the overall intensity of IgA staining (Figures 4A and S4B), a feature also observed in patients with inflammatory bowel diseases (IBD) (van der Waaij et al., 2004). This abundantly coated bacteria profile could reflect differences in the bacterial communities (i.e., large-size bacteria giving stronger signals) or differences in IgA qualities and their binding properties. To distinguish between these possibilities, we sequenced and analyzed bacteria that were sorted as IgA^{neg}, IgA^{int}, and IgA^{hi} from the feces of *Cd3e*$^{-/-}$ mice transferred with different populations of CD4$^+$ T cells or from control (WT) mice (Figure S4A). The identified species from noncoated or coated bacterial fractions (we consider one operational taxonomic unit [OTU] as one species) were used for principal coordinate analysis (PCoA) (Figure 4B). WT mice and *Cd3e*$^{-/-}$ mice transferred with Foxp3$^+$ T cells exhibited a similar profile in which all fecal bacteria or IgA^{neg} groups were substantially separated from IgA^{neg} or IgA$^{int/hi}$ groups or from cecal bacteria. In contrast, in the absence of Foxp3$^+$ T cell regulation (i.e., naive CD4$^+$ T cells transferred alone or along with CD25$^+$*Bcl6*$^{yfp/yfp}$ T cells), there was no clear distinction among IgA^{neg}, IgA^{int}, and IgA^{hi} fractions (Figure 4B). This was confirmed by plotting in Venn graphs, in which the size of circles in the Venn graph reflects the diversity of bacterial species for each fraction (Figures 4C, S4C, and S4D). In mice with Foxp3$^+$ T cell regulation, a smaller percentage of bacterial species overlapped among all the IgA^{hi}, IgA^{int}, and IgA^{neg} fractions, and IgA^{hi} fraction exhibited higher diversity, compared with those in mice without Foxp3$^+$ T cell regulation (Figures 4C, 4D, and S4C).

The less-overlapping profiles correlated with a higher affinity selection index of IgAs, whereas the largely overlapping profiles associated with reduced affinity selection index of IgAs (Figure 3D). To test whether selected and nonselected IgAs differently coat the same bacteria, equal amounts of IgA elicited in the presence or absence of Foxp3$^+$ T cells were tested for binding in vitro against several defined anaerobic bacterial strains isolated from mouse gut. As shown in Figures S4E and S4F,

Figure 3. Foxp3$^+$ T Cell Migration into PP GCs Is Critical for IgA Selection

(A) Representative sections of PPs in *Cd3e*$^{-/-}$ mice transferred with naive CD4$^+$ T cells together with CD25$^+$ WT T cells or CD25$^+$*Bcl6*$^{yfp/yfp}$ T cells stained as indicated and revealing GC B cells and T cells. T cells derived from naive CD4$^+$ T cells appeared in yellow, and the CD25$^+$-derived T cells are stained in green only. The arrows in upper panels indicate the presence of Foxp3-derived Tfh cells, while the arrows in middle panels indicate Tfr cells. Smaller arrows indicate reduced levels of Foxp3 by some Tfr cells.

(B) The percentage and total numbers of the indicated cells in PPs of *Cd3e*$^{-/-}$ mice transferred with naive CD4$^+$ T cells together with CD25$^+$WT T cells or CD25$^+$*Bcl6*$^{yfp/yfp}$ T cells. Mean ± SEM for three to five mice per group.

(C) Flow cytometric profiles of cells from PPs and SILP. B220$^-$IgA$^+$ gate represent plasma cells. Numbers on plots indicate the frequency of cells in the gate.

(D) Total numbers and affinity maturation index of IgA-producing cells from the SILP of WT, *Cd3e*$^{-/-}$, and *Cd3e*$^{-/-}$ transferred with indicated CD4$^+$ T cell subsets. Two to three mice per group, around 50 sequences per mouse were analyzed. R_{CDR}, replacement in CDR1 and CDR2; S_{total}, silent mutations in both CDRs and in framework regions 1 to 3 (FWR1–3).

Two-tailed unpaired Student's t test was used to compare between the indicated mouse groups and (B) *Cd3e*$^{-/-}$ mice transferred with naive CD4$^+$ T cells together with CD25$^+$ WT T cells or (D) WT; ***p < 0.001; N.S., no significant difference. See also Figure S3.

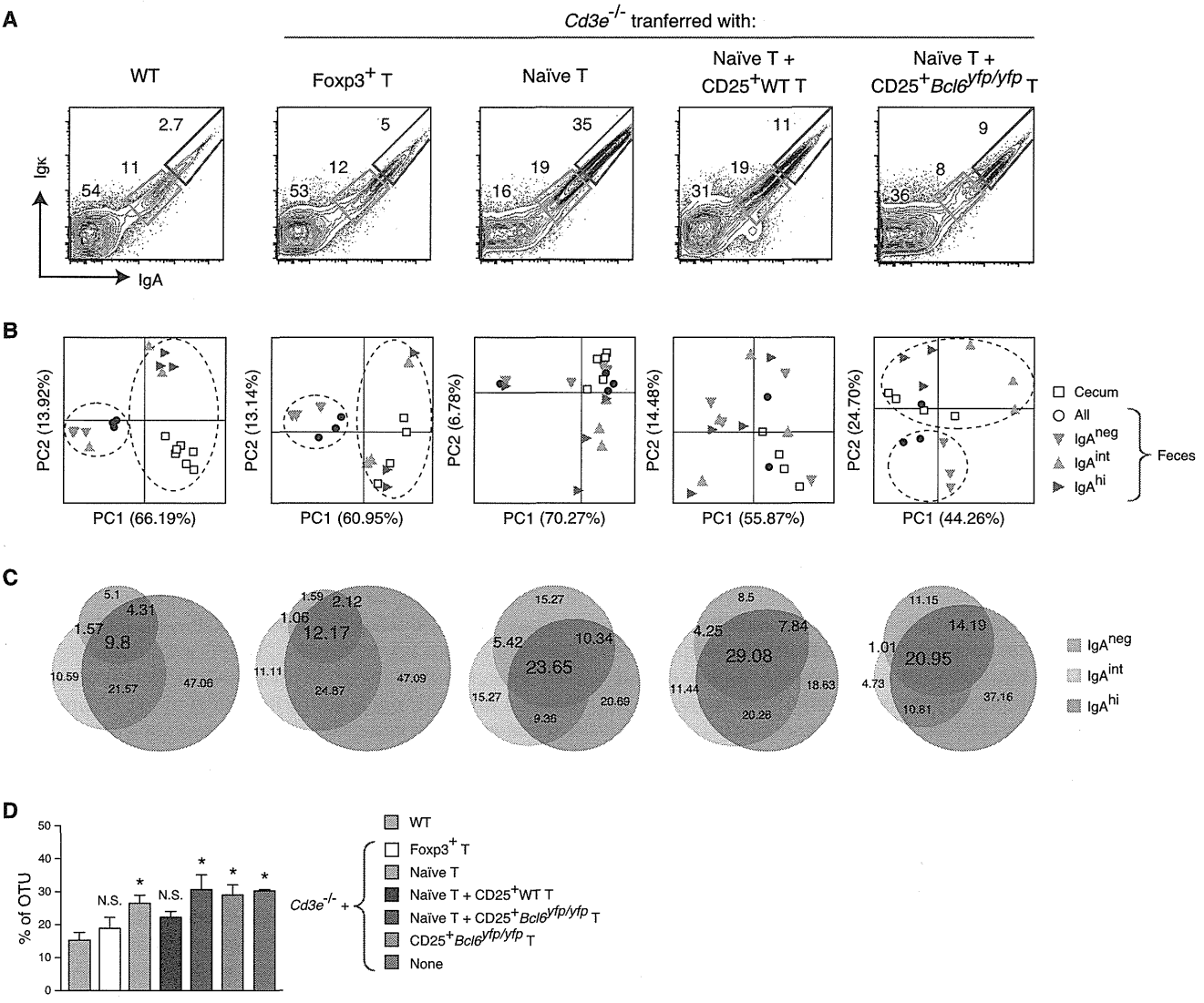

Figure 4. Specific IgA Coating Contributes Maintenance of Microbiota

(A) Representative flow cytometric profiles of fecal bacteria stained as indicated from WT or *Cd3e*$^{-/-}$ mice transferred with indicated CD4$^+$ T cell subsets. Sorting gates for IgA^{neg} (IgA$^-$Igκ$^-$), IgA^{int} (IgA^{int}Igκ^{int}), or IgA^{hi} (IgA^{hi}Igκ^{hi}) are indicated.

(B) Communities clustered by principal coordinate analyses of weighted UniFrac distance of 16S rRNA sequences from total cecal and fecal bacteria, and the IgA^{neg}, IgA^{int}, and IgA^{hi} sorted bacterial fractions from WT or *Cd3e*$^{-/-}$ mice transferred with indicated CD4$^+$ T cell subsets.

(C) Venn diagrams showing the frequencies of bacterial species (OTUs) from the IgA^{neg}, IgA^{int}, and IgA^{hi} sorted bacterial fractions from WT or *Cd3e*$^{-/-}$ mice 10–12 weeks after the transfer of the indicated CD4$^+$ T cell subsets. Data represent one of three to four experiments with consistent results. Numbers represent percentages.

(D) The frequency of OTU overlap among IgA^{neg}, IgA^{int}, and IgA^{hi} sorted bacterial fractions from WT or *Cd3e*$^{-/-}$ mice 10–12 weeks after the transfer of the indicated CD4$^+$ T cell subsets. Mean ± SEM from three to four mice per group. Two-tailed unpaired Student's t test was used to compare between WT and the indicated mouse groups; *$p < 0.05$; N.S., no significant difference.

See also Figure S4.

the nonselected IgAs from mice transferred with naive CD4$^+$ T cells or CD25$^+$*Bcl6*$^{yfp/yfp}$ T cells had higher coating capacity than the IgAs from mice transferred with Foxp3$^+$ T cells. These results suggest that the IgAs generated and selected in the presence of GC Foxp3$^+$ T cells coated moderately and rather specifically a large diversity of bacterial species. This coating might contribute to maintenance rather than elimination of indigenous bacteria to keep the diversity.

Regulation of Immune System by Microbiota

We hypothesized that the presence of very diverse bacterial species would facilitate the perpetual induction of GCs and IgA and the maintenance of Foxp3$^+$ T cell pool in the gut. To test this hypothesis, we performed Mb transplantation experiments. Thus, germ-free (GF) mice were gavaged with Mb harvested from feces of *Cd3e*$^{-/-}$ mice transferred with Foxp3$^+$ T cells (hereafter Foxp3Mb) or naive CD4$^+$ T cells (hereafter Naive4Mb). Mb

harvested from nontransferred *Cd3e*$^{-/-}$ mice (CD3Mb) served as control. The mice were analyzed 2 weeks later. In the PPs, colonization with Foxp3Mb resulted in increase of B cells and T cells, and their activation and differentiation into GC B cells and Tfh cells, respectively (Figures 5A, 5C, S5A, and S5B). Interestingly, the Foxp3Mb induced preferential switching of GC B cells from IgM to IgA, the characteristic gut GC signature. In contrast, Naive4Mb or CD3Mb induced fewer GCs and Tfh cells, with the Naive4Mb supporting B cell class switching to IgG1 rather than to IgA, because of increased IL-4 production by CD4$^+$ T cells located in the PPs of these mice (Figures 5A and 5C). In the SILP, Foxp3Mb generated many more IgA-producing cells and Foxp3$^+$ T cells compared with CD3Mb or Naive4Mb (the latter inducing not Foxp3 but rather T cells secreting IL-4, IL-17, or TNF-α) (Figures 5B, 5D, and S5C). Importantly, the induction of these two characteristic gut homeostatic responses (IgA and Foxp3) by Foxp3Mb associated with a considerably higher diversity of bacterial species compared with mice transplanted with NaiveMb or CD3Mb (Figures 5E and 5F). Because most species correlating with the induction of IgA and Foxp3$^+$ T cells were Firmicutes (Figure S5D) and this phylum contains many spore-forming bacteria, we next performed gavage experiments with the spore fraction from Foxp3Mb (Spore^{Foxp3Mb}). Colonization of GF mice with Spore^{Foxp3Mb} induced GC B cells and Tfh cells that facilitated preferential switching to IgA in the PPs (Figures 5A, 5C, and S5B) and increased the IgA plasma cells compartment and favored the generation or expansion of Foxp3$^+$ T cells in the LP (Figures 5B, 5D, and S5C).

To further evaluate the link between Mb and gut Foxp3$^+$ T cells, we changed the experimental strategy slightly. We first inoculated GF *Cd3e*$^{-/-}$ mice with Foxp3Mb or Naive4Mb and 1 week later transferred Foxp3$^+$ T cells into these mice (Figure 6A). The T cell expansion and B cell responses were assessed 2 weeks after the cell transfer. As shown in Figures S6A and S6B, Foxp3Mb helped the expansion of Foxp3$^+$ T cells in MLN and LP of the SI and LI more vigorously than Naive4Mb. In the PPs, Foxp3Mb but not Naive4Mb facilitated the activation and differentiation of Foxp3$^+$ T cells into Tfh cells with GC and IgA-inducing properties (Figures 6A and 6B; Tsuji et al., 2009). Thus, Foxp3Mb promoted maturation of the gut immune system and exhibited robust Foxp3 and IgA-supportive properties in gut.

Dominant Immune-Regulatory Role of Foxp3Mb

To further evaluate the features of Foxp3Mb in more competitive settings, we performed experiments with specific-pathogen-free (SPF) young mice. Thus, 3-week-old WT mice were colonized by fur painting with Foxp3Mb. Adult WTMb, CD3Mb, or Naive4Mb mice were used for comparison. Strikingly, even in competitive situations, the Foxp3Mb (or a similarly complex and balanced adult WTMb) had IgA-inducing properties (Figure 7A). Indeed, compared with noninfected mice, the Foxp3Mb induced a substantial increase in frequencies and numbers of GCs and IgAs in PPs (Figures 7A and 7B). Naive4Mb or CD3Mb induced activation and IgA differentiation in PPs, but to a much more limited degree than Foxp3Mb or WTMb. Yet, the IgA production was increased when Naive4Mb was mixed with Foxp3Mb (Figures 7A and 7B). The results clearly demonstrated the prevalent IgA-inducing properties of Foxp3Mb. They also confirmed the potential of Mb selected and maintained by the immunocompetant host to dominantly regulate postnatal maturation of the immune system.

DISCUSSION

In this manuscript we have revealed that (1) differentiation of Foxp3$^+$ T cells into Tfr cells is required for the IgA's selection in GCs; (2) the amount and quality of IgAs directly influence the diversity and phylogenetic structure of bacterial communities; (3) rich and balanced Mb induce maturation of the gut immune system by promoting Foxp3$^+$ T cells and IgAs; and (4) in turn, the Foxp3$^+$ T cells and IgAs, through controlled diversification of stimulatory bacterial species, establish a self-regulatory loop mediating host-bacterial mutualism. Thus, it appears that the adaptive immune system contributes to the maintenance, rather than elimination, of complex microbial communities that probably enrich the genomic and metabolic capacity of the host, which is required for gut homeostasis and health.

Multiple studies revealed the importance of balanced Mb for the maintenance of gut barrier and immune homeostasis. Biased expansion of certain bacterial species impairs epithelial barrier and induces excessive activation of the immune system and generation of T cell subsets with inflammatory properties (Fagarasan et al., 2010; Kamada et al., 2013; Kawamoto et al., 2012; Littman and Pamer, 2011). Furthermore, reduced microbiome richness when accompanied by inflammatory phenotypes also associates with obesity, insulin resistance, and dyslipidemia (Karlsson et al., 2013; Le Chatelier et al., 2013; Qin et al., 2012). We demonstrated that the acquired arm of the immune system impacts considerably the diversity and phylogenetic structure of microbial communities in the gut.

We showed that Foxp3$^+$ T cell migration and differentiation into Tfr cells in the GCs is critical for IgA selection. The lack of Tfr cells associates with increased number of Tfh cells that license not only the mutated, presumably high-affinity, but also the germline and less mutated (and presumably poly- and/or self-reactive) B cells to emerge from the GCs, as previously reported (Baumjohann et al., 2013; Good-Jacobson et al., 2010; Kawamoto et al., 2012; Linterman et al., 2011; Vinuesa et al., 2013). In the absence of Tfr cell regulation, Tfh cells had skewed helper properties (e.g., due to production of different cytokines). The Tfh cell phenotype in GCs lacking Tfr cells may reflect not only the lack of direct suppressive effects of Tfr cells on Tfh cells, but also the downstream events resulting from deregulation of GCs.

Thus, it is highly likely that defective selection of IgAs leading to microbial changes would affect the generation of bacterial metabolic products that are required for induction of gut effector T cell subsets, like Foxp3$^+$, RORγt$^+$, or Foxp3$^+$RORγt$^+$ T cells (Atarashi et al., 2011, 2013; Ivanov et al., 2009; Lochner et al., 2008; Zhou et al., 2008). For example, short-chain fatty acids (SCFAs), especially butyric acid, derived from fermentation of dietary fibers by certain bacterial species (e.g., *Clostridia*), appear to facilitate the induction and expansion of Foxp3$^+$ T cells in gut through epigenetic changes (Arpaia et al., 2013; Furusawa et al., 2013; Smith et al., 2013). We also observed that a reduced bacterial diversity in *Cd3e*$^{-/-}$ mice coincided with lower intestinal amounts of SCFAs (including acetate, propionate, or butyrate)

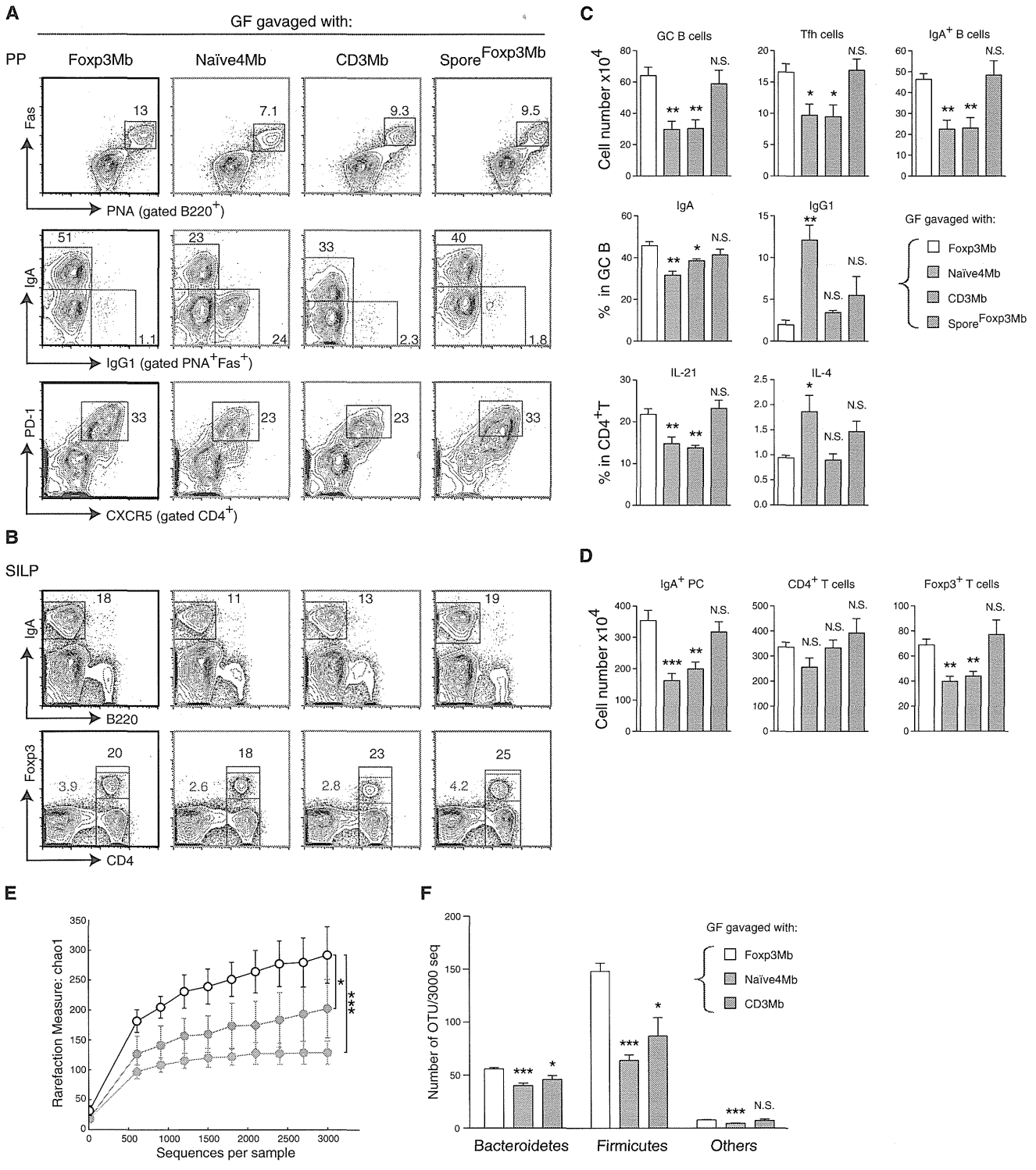

Figure 5. Foxp3-Regulated Microbiota Induces Maturation of Gut Immune System

(A–D) Flow cytometric profiles of (A) PP cells and (B) SILP stained as indicated and total numbers of indicated cell populations from (C) PPs and (D) SILP of GF mice gavaged with fresh microbiota obtained from *Cd3e*$^{-/-}$ mice transferred with naive CD4$^+$ T cells (Naive4Mb) or Foxp3$^+$ T cells (Foxp3Mb), or nontransferred *Cd3e*$^{-/-}$ mice (CD3Mb) as control. Gavage with spore fraction obtained from Foxp3Mb is also shown. Feces were obtained 10–12 weeks after T cell transfer. Mice were analyzed 2 weeks after bacterial transplantation. Data represent one of the three experiments with consistent results. At least four mice per group were analyzed.

(legend continued on next page)

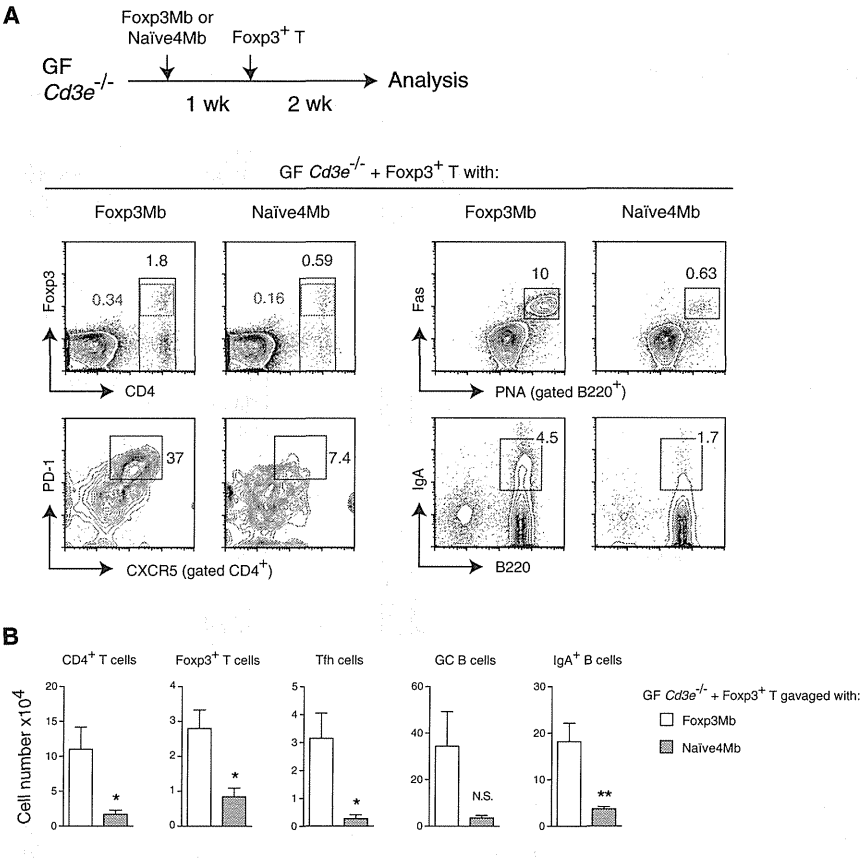

Figure 6. Foxp3-Regulated Microbiota Has Foxp3-Supportive Properties

(A) Scheme of the transfer experiment with GF *Cd3e*$^{-/-}$ mice and flow cytometric profiles of cells isolated from PPs of GF *Cd3e*$^{-/-}$ mice gavaged with fresh microbiota obtained from transferred mice and injected with Foxp3$^+$ T cells as indicated in scheme and stained for the indicated markers. Numbers indicate the frequency of cells in the gate. Data represent one of the two experiments with consistent results. At least four mice per group were analyzed.

(B) Total numbers of CD4$^+$ T, Foxp3$^+$ T, Tfh, GC B, and IgA$^+$ B cells in PP obtained from the indicated mice. Mean ± SEM in bar graphs for four mice per group. Two-tailed unpaired Student's t test was used to compare between these groups; $^{**}p < 0.01$; $^{*}p < 0.05$; N.S., no significant difference. See also Figure S6.

and that these levels recovered upon reconstitution of mice with Foxp3$^+$ T cells and normalization of Mb (data not shown). Additional microbial-derived metabolites are probably modulating other subsets of T cells, which upon activation and interaction with B cells could convert into GC Tfh cells with distinct helper characteristics (Hirota et al., 2013; Takahashi et al., 2012; Tsuji et al., 2009).

The Foxp3-IgA module probably involves complex feedback and feed-forward loops between Mb and immune cells that extend well beyond mucosal immune system (Fagarasan et al., 2002; Suzuki et al., 2004; Wei et al., 2011). For example, when Foxp3 control of GCs was missing (i.e., *Cd3e*$^{-/-}$ mice cotransferred with naive and CD25$^+$*Bcl6*$^{yfp/yfp}$ T cells), we observed a higher ratio of Firmicutes to Bacteroidetes even in the absence of overt inflammation. This shift associates with a considerable increased body weight, suggesting alterations in energy harvest and metabolism (Turnbaugh et al., 2006). In contrast, in the complete absence of Foxp3$^+$ T cells, there was a pronounced reduction of Firmicutes, which together with expansion of Proteobacteria could account for the decreased weight observed in such mice with overt inflammation (Elson and Cong, 2012).

We revealed that reduced diversification and affinity maturation of IgAs in the GCs associated with abundant coating of bacteria with largely nonspecific IgAs and reduced diversity and skewed gut Mb. Conversely, diversified and well-selected IgA repertoires in GCs associated not only with specific bacteria coating but also with rich and balanced bacterial communities. These observations suggest that bacteria coating by highly diversified and selected IgAs contributes to maintenance rather than elimination of indigenous bacteria, thus increasing the diversity and stability of Mb. It is accepted that IgA can control infection by coating pathogenic bacteria and preventing their contact to the gut epithelium, a process called immune exclusion (Strugnell and Wijburg, 2010). However, IgA coating of commensal bacteria might promote changes in the bacteria itself, such as modification in the bacterial gene expression (Peterson et al., 2007), influencing their metabolic processes as well as their biogeography, proliferation, and survival within the gut. There might be multiple mechanisms (which may work differently depending on the bacteria type, its growth stage and location, and available dietary components) by which IgA binding controls the Mb, but these remain to be elucidated in future studies.

Our study raises the question as to whether different types of Mb are "seen" differently by the immune system and, if so, whether they trigger distinct type of immune responses. We found that a complex and balanced Mb promptly elicits immune responses with typical mucosal characteristics, namely induction of GCs with IgA-supporting properties, and induction or expansion of CD4$^+$ T cells, especially of Foxp3$^+$ T cells. In contrast, a poor and skewed Mb provokes responses with mixed mucosal and systemic characteristics (i.e., GC

(E and F) Diversity of bacterial species (>97% identity) (E) and numbers of OTUs/3,000 sequences (F) in cecal contents from GF mice gavaged with the indicated microbiota; mean ± SEM from four to six mice per group. Two-tailed unpaired Student's t test was used to compare between the GF mice gavaged with Foxp3Mb and the indicated mouse groups; $^{***}p < 0.001$; $^{*}p < 0.05$; N.S., no significant difference.
See also Figure S5.

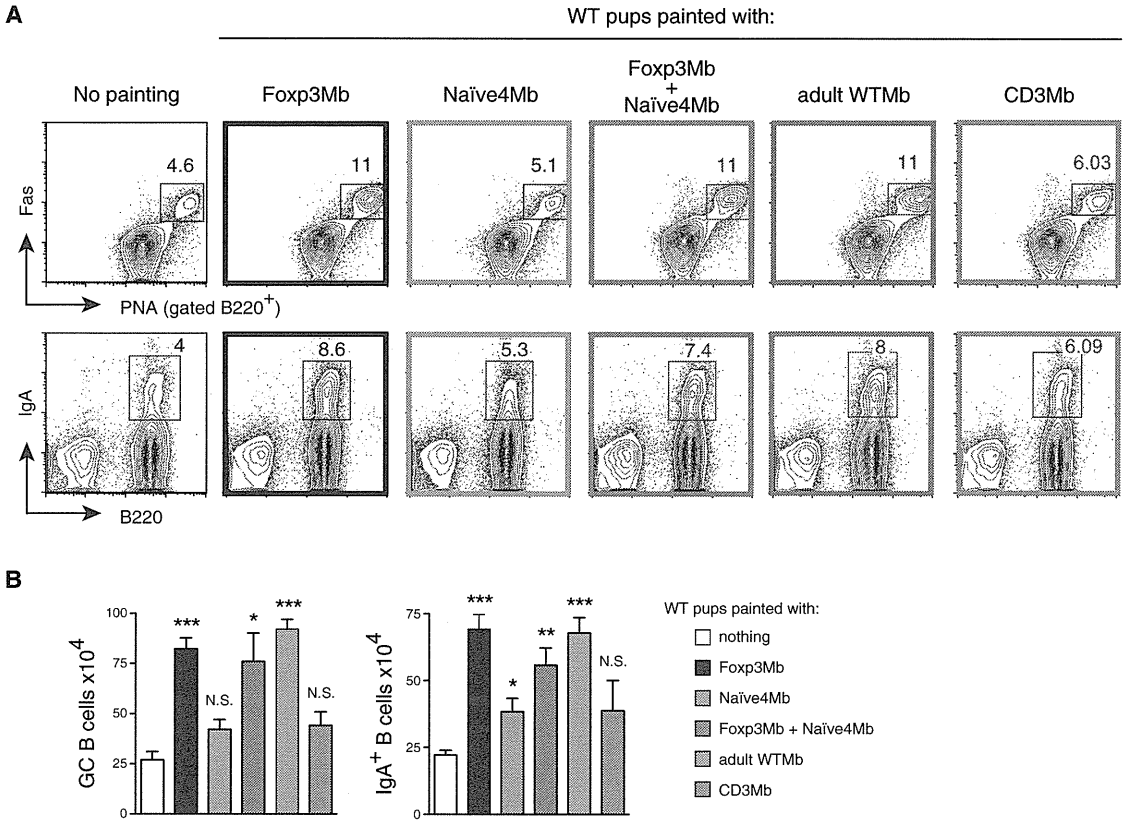

Figure 7. Dominant Effect of Foxp3-Regulated Microbiota

(A) Representative flow cytometric profiles of cells from PPs of WT pups "painted" with fecal extracts from adult WT mice (adult WTMb), nontransferred *Cd3e*$^{-/-}$ mice (CD3Mb), or the *Cd3e*$^{-/-}$ mice transferred with naive CD4$^+$ T cells (Naive4Mb) or Foxp3$^+$ T cells (Foxp3Mb). Fecal extracts from two to four mice per group were pooled 10–12 weeks after T cell transfer, and host mice were analyzed 2 weeks after the painting. Numbers indicate the frequency of cells in the gates. Data represent one of the three experiments with consistent results. At least four mice per group were analyzed.

(B) Total numbers of GC B cells and IgA$^+$ B cells from the PPs of indicated mice. Mean ± SEM for three to five mice per group. Two-tailed unpaired Student's t test was used to compare between nonpainted and the indicated mouse groups; ***$p < 0.001$; **$p < 0.01$; *$p < 0.05$; N.S., no significant difference.

B cells switching not only to IgA but also to IgG1, and possibly to IgE). These observations suggest that the immune system recognizes complex and balanced microbial communities as "gut Mb signature" and respond by adaptations that foster the maintenance of such complex bacterial structures. An increased diversity probably enhances the stability of Mb potentiating its metabolic capacity, in parallel with exerting a constant yet controllable pressure for diversification and fitness of the immune system. In contrast, poor and skewed bacterial communities might be recognized as having pathogenic treats and as such elicit systemic type of responses that in certain conditions could lead to autoimmune diseases or allergies. Thus, the acquisition of Foxp3, IgA, and its secretory mechanisms, and the development of complex GALT structures that facilitate coordinated and controlled immune-receptor diversification seem adaptations that allowed vertebrates to establish symbiotic relationships with Mb and to become an evolutionary success.

The results presented here should be useful when considering strategies to reestablish symbiosis in intestinal pathologies caused by various immunodeficiencies and associated with gut inflammation.

EXPERIMENTAL PROCEDURES

Mice

C57BL/6 germ-free (GF) mice were initially purchased from Sankyo Laboratories Japan and were bred and maintained in vinyl isolators in the animal facility at IMS-RCAI, RIKEN Yokohama. 5-week-old GF mice were used for microbiota transplantation experiments. Other mice, like wild-type (WT), *Cd3e*$^{-/-}$ (Malissen et al., 1995), *Ighm*$^{-/-}$, *Rag1*$^{-/-}$, *Foxp3*^{EGFP} (Ly5.1 or 5.2) (Wang et al., 2008), *Bcl6*$^{yfp/yfp}$ (Kitano et al., 2011), and *Aicda*$^{-/-}$, were on a C57BL/6 background, bred and maintained in SPF facility at IMS-RCAI. All animal experiments were performed in accordance with approved protocols from the Institutional Animal Care at RIKEN. Littermate information of immunodeficient mice is described in Supplemental Experimental Procedures.

IgA$^+$ Cell Sorting, IgA Heavy Chain Gene Sequencing, and Mutational Analyses

Single B220$^-$IgA$^+$ plasma cells from lamina propria of small intestine (SILP) were sorted into 96-well PCR plates containing 10 μl of 50 μg/ml yeast tRNA as carrier, using FACS Aria cell sorter (Becton Dickinson). The method for IgA heavy chain gene sequence analyses was previously described (Hershberg et al., 2008; Kawamoto et al., 2012).

Histological Analysis

For immunohistochemical analysis, small intestine samples were fixed and stained as previously described (Kawamoto et al., 2012). Before Foxp3

staining, formaldehyde-fixed sections were treated with HistoVT One (Nacalai Tesque) at 70°C for 20 min for antigen retrieval. For hematoxylin-eosin (HE) staining, large intestine samples were fixed and stained with HE (Muto Pure Chemicals) according to the manufacturer's protocol. The stained slides were examined with a Zeiss Axioplan 2 fluorescence microscope.

Assessment of Intestinal Inflammation

Mice were sacrificed usually around 10–12 weeks after the transfer of T cells. Distal colons were fixed with 4% paraformaldehyde and stained with hematoxylin and eosin. The degree of intestinal inflammation was graded from 0 to 3 for the four following criteria: degree of epithelial hyperplasia and goblet cell depletion; leukocyte infiltration in the lamina propria; area of tissue affected; and the presence of markers of severe inflammation such as crypt abscesses and submucosal inflammation (Izcue et al., 2008). Scores for each of the criteria were added to give a total score of 0 to 12 for each sample. The total colonic score was calculated as the average of the individual scores from several sections per mouse.

Fecal Suspension for Microbiota Reconstitution

Fecal pellets were collected from C57BL/6 or from T-cell-transferred *Cd3e*$^{-/-}$ mice and suspended with sterile PBS (5–7 feces/3 ml PBS). Bacteria number in fecal suspension was counted by Flow-Check Fluorospheres (Beckman Coulter) with FACS CantoII (Becton Dickinson) and adjusted to same number in each sample. The spore fraction was prepared as described previously (Atarashi et al., 2013).

Germ-free WT Mice Experiments

Germ-free C57BL/6 mice were transferred into autoclaved sterile cages and gavaged with 100 μl of fecal suspension from the *Cd3e*$^{-/-}$ mice transferred with Foxp3^{+} T cells, naive CD4^{+} T cells, or nontransferred *Cd3e*$^{-/-}$ mice. At 2 weeks after gavage, mice were analyzed and cecum contents were collected for bacterial DNA sequencing.

Germ-free *Cd3e*$^{-/-}$ Mice Experiments

Germ-free *Cd3e*$^{-/-}$ mice were gavaged with fecal suspension from the *Cd3e*$^{-/-}$ mice transferred with Foxp3^{+} T cells or naive CD4^{+} T cells. After 1 week, 2 × 10^{5} CD4^{+}GFP^{+} (Foxp3^{+}) T cells sorted from spleen and LNs of Foxp3^{EGFP} mice were injected intravenously. The recipient mice were analyzed 2 weeks after the Foxp3^{+} T cell transfer.

Fur-Painting of SPF Mice

For painting experiments, 3-week-old female C57BL/6 mice purchased from CLEA Japan had fecal suspension from different mice painted on their fur. Mice were analyzed 2 weeks after the painting.

Evaluation of IgA-Coated Bacteria by Flow Cytometry

Flow cytometric analysis of bacteria was performed as described (van der Waaij et al., 1996) with some modifications. Detailed procedure is described in Supplemental Experimental Procedures.

Sorting of IgA-Coated Fecal Bacteria

Fecal bacteria were stained as described above and purified on a FACSAria (Becton Dickinson) cell sorter as IgA^{neg} (IgA^{-}Igκ^{-}), IgA^{int} (IgA^{int}Igκ^{int}), or IgA^{hi} (IgA^{hi}Igκ^{hi}) cells. Sorted bacteria were centrifuged at 12,000 × *g* for 10 min and bacterial pellet was stored at –80°C until use. Bacterial genomic DNA was purified with conventional phenol:chloroform extraction followed by ethanol precipitation. 16*S* rRNA genes were amplified and analyzed as described below.

Preparation of DNA and Pyrosequencing

Cecum and stool samples were stored at –80°C until use. DNA was purified with the QIAamp DNA stool mini kit (QIAGEN) according with manufacturer's instructions with a high-temperature incubation option. DNA samples were amplified using V1–V2 region primers targeting bacterial 16*S* rRNA genes with Roche 454 Lib-L pyrosequencing adaptor and barcode sequence as previously described (Kawamoto et al., 2012). PCR products were cleaned by Wizard SV Gel and PCR Clean-up system (Promega) and sequencing was carried out by with a 454 GS Junior pyrosequencer (Roche).

16S rRNA Data Processing and Analysis

Sequences were processed and analyzed with QIIME pipeline (Caporaso et al., 2010). Detailed procedure is described in Supplemental Experimental Procedures.

ACCESSION NUMBERS

The bacterial 16S rRNA amplicon sequence data are available in DNA Data Bank of Japan (DDBJ) under the accession number PRJDB2881.

SUPPLEMENTAL INFORMATION

Supplemental Information includes six figures and Supplemental Experimental Procedures and can be found with this article online at http://dx.doi.org/10.1016/j.immuni.2014.05.016.

AUTHOR CONTRIBUTIONS

S.K. conducted all mice experiments and analysis. M.M. conducted the bacterial 16S rRNA pyrosequencing, data processing, and analysis. L.M.K. conducted IgA mutational analyses, evaluation, and sorting of IgA-coated fecal bacteria. W.S. and M.H. provided help for 16S rRNA data analysis. K.A. and K.H. provided help for isolation and culture of bacterial strains from mouse cecum. Y.D., Y.T., and H.Q. provided help for mice experiment and Y.D. provided help with IgA heavy chain gene sequencing. T.O. provided *Bcl6*$^{yfp/yfp}$ mice. S.K., M.M., L.M.K., and S.F. interpreted the data and wrote the manuscript. S.F. designed and supervised the study.

ACKNOWLEDGMENTS

We thank T. Honjo, O. Kanagawa, I. Taniuchi, and D. Littman for inspiring discussions, suggestions, and critical comments and M. Miyajima, K. Suzuki, K. Moro, A. Hijikata, H. Fujimoto, Y. Hachiman, Y. Murahashi, C. Shindo, K. Komiya, H. Kuroyanagi, E. Iioka, Y. Takayama, E. Ohmori, M. Kiuchi, and Y. Hattori for technical assistance. The data reported in this paper are tabulated in the main paper and the Supplemental Data. This work was supported in part by Grants-in-Aid for Scientific Research (25293118) (S.F.) and for Young Scientist (25860375), the Naito Foundation, RIKEN special Postdoctoral Researchers Program (S.K.), the global COE project "Genome Information Big Bang" from the MEXT of Japan (M.H.), and JSPS Postdoctoral Fellowship for Foreign Researchers (L.M.K.).

Received: December 30, 2013
Accepted: May 9, 2014
Published: July 10, 2014

REFERENCES

Arpaia, N., Campbell, C., Fan, X., Dikiy, S., van der Veeken, J., deRoos, P., Liu, H., Cross, J.R., Pfeffer, K., Coffer, P.J., and Rudensky, A.Y. (2013). Metabolites produced by commensal bacteria promote peripheral regulatory T-cell generation. Nature *504*, 451–455.

Atarashi, K., Tanoue, T., Shima, T., Imaoka, A., Kuwahara, T., Momose, Y., Cheng, G., Yamasaki, S., Saito, T., Ohba, Y., et al. (2011). Induction of colonic regulatory T cells by indigenous Clostridium species. Science *331*, 337–341.

Atarashi, K., Tanoue, T., Oshima, K., Suda, W., Nagano, Y., Nishikawa, H., Fukuda, S., Saito, T., Narushima, S., Hase, K., et al. (2013). Treg induction by a rationally selected mixture of Clostridia strains from the human microbiota. Nature *500*, 232–236.

Baumjohann, D., Preite, S., Reboldi, A., Ronchi, F., Ansel, K.M., Lanzavecchia, A., and Sallusto, F. (2013). Persistent antigen and germinal center B cells sustain T follicular helper cell responses and phenotype. Immunity *38*, 596–605.

Caporaso, J.G., Kuczynski, J., Stombaugh, J., Bittinger, K., Bushman, F.D., Costello, E.K., Fierer, N., Peña, A.G., Goodrich, J.K., Gordon, J.I., et al. (2010). QIIME allows analysis of high-throughput community sequencing data. Nat. Methods *7*, 335–336.

Chung, Y., Tanaka, S., Chu, F., Nurieva, R.I., Martinez, G.J., Rawal, S., Wang, Y.H., Lim, H., Reynolds, J.M., Zhou, X.H., et al. (2011). Follicular regulatory T cells expressing Foxp3 and Bcl-6 suppress germinal center reactions. Nat. Med. *17*, 983–988.

Cong, Y., Feng, T., Fujihashi, K., Schoeb, T.R., and Elson, C.O. (2009). A dominant, coordinated T regulatory cell-IgA response to the intestinal microbiota. Proc. Natl. Acad. Sci. USA *106*, 19256–19261.

Elson, C.O., and Cong, Y. (2012). Host-microbiota interactions in inflammatory bowel disease. Gut Microbes *3*, 332–344.

Fagarasan, S., Muramatsu, M., Suzuki, K., Nagaoka, H., Hiai, H., and Honjo, T. (2002). Critical roles of activation-induced cytidine deaminase in the homeostasis of gut flora. Science *298*, 1424–1427.

Fagarasan, S., Kawamoto, S., Kanagawa, O., and Suzuki, K. (2010). Adaptive immune regulation in the gut: T cell-dependent and T cell-independent IgA synthesis. Annu. Rev. Immunol. *28*, 243–273.

Furusawa, Y., Obata, Y., Fukuda, S., Endo, T.A., Nakato, G., Takahashi, D., Nakanishi, Y., Uetake, C., Kato, K., Kato, T., et al. (2013). Commensal microbe-derived butyrate induces the differentiation of colonic regulatory T cells. Nature *504*, 446–450.

Geuking, M.B., Cahenzli, J., Lawson, M.A., Ng, D.C., Slack, E., Hapfelmeier, S., McCoy, K.D., and Macpherson, A.J. (2011). Intestinal bacterial colonization induces mutualistic regulatory T cell responses. Immunity *34*, 794–806.

Good-Jacobson, K.L., Szumilas, C.G., Chen, L., Sharpe, A.H., Tomayko, M.M., and Shlomchik, M.J. (2010). PD-1 regulates germinal center B cell survival and the formation and affinity of long-lived plasma cells. Nat. Immunol. *11*, 535–542.

Hershberg, U., Uduman, M., Shlomchik, M.J., and Kleinstein, S.H. (2008). Improved methods for detecting selection by mutation analysis of Ig V region sequences. Int. Immunol. *20*, 683–694.

Hirota, K., Turner, J.E., Villa, M., Duarte, J.H., Demengeot, J., Steinmetz, O.M., and Stockinger, B. (2013). Plasticity of Th17 cells in Peyer's patches is responsible for the induction of T cell-dependent IgA responses. Nat. Immunol. *14*, 372–379.

Hooper, L.V., Littman, D.R., and Macpherson, A.J. (2012). Interactions between the microbiota and the immune system. Science *336*, 1268–1273.

Ivanov, I.I., Atarashi, K., Manel, N., Brodie, E.L., Shima, T., Karaoz, U., Wei, D., Goldfarb, K.C., Santee, C.A., Lynch, S.V., et al. (2009). Induction of intestinal Th17 cells by segmented filamentous bacteria. Cell *139*, 485–498.

Izcue, A., Coombes, J.L., and Powrie, F. (2006). Regulatory T cells suppress systemic and mucosal immune activation to control intestinal inflammation. Immunol. Rev. *212*, 256–271.

Izcue, A., Hue, S., Buonocore, S., Arancibia-Cárcamo, C.V., Ahern, P.P., Iwakura, Y., Maloy, K.J., and Powrie, F. (2008). Interleukin-23 restrains regulatory T cell activity to drive T cell-dependent colitis. Immunity *28*, 559–570.

Johnston, R.J., Poholek, A.C., DiToro, D., Yusuf, I., Eto, D., Barnett, B., Dent, A.L., Craft, J., and Crotty, S. (2009). Bcl6 and Blimp-1 are reciprocal and antagonistic regulators of T follicular helper cell differentiation. Science *325*, 1006–1010.

Josefowicz, S.Z., Niec, R.E., Kim, H.Y., Treuting, P., Chinen, T., Zheng, Y., Umetsu, D.T., and Rudensky, A.Y. (2012). Extrathymically generated regulatory T cells control mucosal TH2 inflammation. Nature *482*, 395–399.

Kamada, N., Seo, S.U., Chen, G.Y., and Núñez, G. (2013). Role of the gut microbiota in immunity and inflammatory disease. Nat. Rev. Immunol. *13*, 321–335.

Karlsson, F.H., Tremaroli, V., Nookaew, I., Bergström, G., Behre, C.J., Fagerberg, B., Nielsen, J., and Bäckhed, F. (2013). Gut metagenome in European women with normal, impaired and diabetic glucose control. Nature *498*, 99–103.

Kau, A.L., Ahern, P.P., Griffin, N.W., Goodman, A.L., and Gordon, J.I. (2011). Human nutrition, the gut microbiome and the immune system. Nature *474*, 327–336.

Kawamoto, S., Tran, T.H., Maruya, M., Suzuki, K., Doi, Y., Tsutsui, Y., Kato, L.M., and Fagarasan, S. (2012). The inhibitory receptor PD-1 regulates IgA selection and bacterial composition in the gut. Science *336*, 485–489.

Kitano, M., Moriyama, S., Ando, Y., Hikida, M., Mori, Y., Kurosaki, T., and Okada, T. (2011). Bcl6 protein expression shapes pre-germinal center B cell dynamics and follicular helper T cell heterogeneity. Immunity *34*, 961–972.

Le Chatelier, E., Nielsen, T., Qin, J., Prifti, E., Hildebrand, F., Falony, G., Almeida, M., Arumugam, M., Batto, J.M., Kennedy, S., et al.; MetaHIT consortium (2013). Richness of human gut microbiome correlates with metabolic markers. Nature *500*, 541–546.

Linterman, M.A., Pierson, W., Lee, S.K., Kallies, A., Kawamoto, S., Rayner, T.F., Srivastava, M., Divekar, D.P., Beaton, L., Hogan, J.J., et al. (2011). Foxp3+ follicular regulatory T cells control the germinal center response. Nat. Med. *17*, 975–982.

Littman, D.R., and Pamer, E.G. (2011). Role of the commensal microbiota in normal and pathogenic host immune responses. Cell Host Microbe *10*, 311–323.

Lochner, M., Peduto, L., Cherrier, M., Sawa, S., Langa, F., Varona, R., Riethmacher, D., Si-Tahar, M., Di Santo, J.P., and Eberl, G. (2008). In vivo equilibrium of proinflammatory IL-17+ and regulatory IL-10+ Foxp3+ RORgamma t+ T cells. J. Exp. Med. *205*, 1381–1393.

Malissen, M., Gillet, A., Ardouin, L., Bouvier, G., Trucy, J., Ferrier, P., Vivier, E., and Malissen, B. (1995). Altered T cell development in mice with a targeted mutation of the CD3-epsilon gene. EMBO J. *14*, 4641–4653.

Manichanh, C., Rigottier-Gois, L., Bonnaud, E., Gloux, K., Pelletier, E., Frangeul, L., Nalin, R., Jarrin, C., Chardon, P., Marteau, P., et al. (2006). Reduced diversity of faecal microbiota in Crohn's disease revealed by a metagenomic approach. Gut *55*, 205–211.

Maynard, C.L., Elson, C.O., Hatton, R.D., and Weaver, C.T. (2012). Reciprocal interactions of the intestinal microbiota and immune system. Nature *489*, 231–241.

Nicholson, J.K., Holmes, E., Kinross, J., Burcelin, R., Gibson, G., Jia, W., and Pettersson, S. (2012). Host-gut microbiota metabolic interactions. Science *336*, 1262–1267.

Nishikawa, J., Kudo, T., Sakata, S., Benno, Y., and Sugiyama, T. (2009). Diversity of mucosa-associated microbiota in active and inactive ulcerative colitis. Scand. J. Gastroenterol. *44*, 180–186.

Nurieva, R.I., Chung, Y., Martinez, G.J., Yang, X.O., Tanaka, S., Matskevitch, T.D., Wang, Y.H., and Dong, C. (2009). Bcl6 mediates the development of T follicular helper cells. Science *325*, 1001–1005.

Ott, S.J., Musfeldt, M., Wenderoth, D.F., Hampe, J., Brant, O., Fölsch, U.R., Timmis, K.N., and Schreiber, S. (2004). Reduction in diversity of the colonic mucosa associated bacterial microflora in patients with active inflammatory bowel disease. Gut *53*, 685–693.

Peterson, D.A., McNulty, N.P., Guruge, J.L., and Gordon, J.I. (2007). IgA response to symbiotic bacteria as a mediator of gut homeostasis. Cell Host Microbe *2*, 328–339.

Qin, J., Li, Y., Cai, Z., Li, S., Zhu, J., Zhang, F., Liang, S., Zhang, W., Guan, Y., Shen, D., et al. (2012). A metagenome-wide association study of gut microbiota in type 2 diabetes. Nature *490*, 55–60.

Smith, P.M., Howitt, M.R., Panikov, N., Michaud, M., Gallini, C.A., Bohlooly-Y, M., Glickman, J.N., and Garrett, W.S. (2013). The microbial metabolites, short-chain fatty acids, regulate colonic Treg cell homeostasis. Science *341*, 569–573.

Strugnell, R.A., and Wijburg, O.L. (2010). The role of secretory antibodies in infection immunity. Nat. Rev. Microbiol. *8*, 656–667.

Sutherland, D.B., and Fagarasan, S. (2012). IgA synthesis: a form of functional immune adaptation extending beyond gut. Curr. Opin. Immunol. *24*, 261–268.

Suzuki, K., Meek, B., Doi, Y., Muramatsu, M., Chiba, T., Honjo, T., and Fagarasan, S. (2004). Aberrant expansion of segmented filamentous bacteria in IgA-deficient gut. Proc. Natl. Acad. Sci. USA *101*, 1981–1986.

Takahashi, H., Kanno, T., Nakayamada, S., Hirahara, K., Sciumè, G., Muljo, S.A., Kuchen, S., Casellas, R., Wei, L., Kanno, Y., and O'Shea, J.J. (2012). TGF-β and retinoic acid induce the microRNA miR-10a, which targets Bcl-6 and constrains the plasticity of helper T cells. Nat. Immunol. *13*, 587–595.

Tsuji, M., Komatsu, N., Kawamoto, S., Suzuki, K., Kanagawa, O., Honjo, T., Hori, S., and Fagarasan, S. (2009). Preferential generation of follicular B

helper T cells from Foxp3+ T cells in gut Peyer's patches. Science *323*, 1488–1492.

Turnbaugh, P.J., Ley, R.E., Mahowald, M.A., Magrini, V., Mardis, E.R., and Gordon, J.I. (2006). An obesity-associated gut microbiome with increased capacity for energy harvest. Nature *444*, 1027–1031.

van der Waaij, L.A., Limburg, P.C., Mesander, G., and van der Waaij, D. (1996). In vivo IgA coating of anaerobic bacteria in human faeces. Gut *38*, 348–354.

van der Waaij, L.A., Kroese, F.G., Visser, A., Nelis, G.F., Westerveld, B.D., Jansen, P.L., and Hunter, J.O. (2004). Immunoglobulin coating of faecal bacteria in inflammatory bowel disease. Eur. J. Gastroenterol. Hepatol. *16*, 669–674.

Vinuesa, C.G., Fagarasan, S., and Dong, C. (2013). New territory for T follicular helper cells. Immunity *39*, 417–420.

Wang, Y., Kissenpfennig, A., Mingueneau, M., Richelme, S., Perrin, P., Chevrier, S., Genton, C., Lucas, B., DiSanto, J.P., Acha-Orbea, H., et al. (2008). Th2 lymphoproliferative disorder of LatY136F mutant mice unfolds independently of TCR-MHC engagement and is insensitive to the action of Foxp3+ regulatory T cells. J. Immunol. *180*, 1565–1575.

Wei, M., Shinkura, R., Doi, Y., Maruya, M., Fagarasan, S., and Honjo, T. (2011). Mice carrying a knock-in mutation of Aicda resulting in a defect in somatic hypermutation have impaired gut homeostasis and compromised mucosal defense. Nat. Immunol. *12*, 264–270.

Wollenberg, I., Agua-Doce, A., Hernández, A., Almeida, C., Oliveira, V.G., Faro, J., and Graca, L. (2011). Regulation of the germinal center reaction by Foxp3+ follicular regulatory T cells. J. Immunol. *187*, 4553–4560.

Yu, D., Rao, S., Tsai, L.M., Lee, S.K., He, Y., Sutcliffe, E.L., Srivastava, M., Linterman, M., Zheng, L., Simpson, N., et al. (2009). The transcriptional repressor Bcl-6 directs T follicular helper cell lineage commitment. Immunity *31*, 457–468.

Zhou, L., Lopes, J.E., Chong, M.M., Ivanov, I.I., Min, R., Victora, G.D., Shen, Y., Du, J., Rubtsov, Y.P., Rudensky, A.Y., et al. (2008). TGF-beta-induced Foxp3 inhibits T(H)17 cell differentiation by antagonizing RORgammat function. Nature *453*, 236–240.

nature immunology

The epigenetic regulator Uhrf1 facilitates the proliferation and maturation of colonic regulatory T cells

Yuuki Obata[1–4,18], Yukihiro Furusawa[1,3,17,18], Takaho A Endo[5], Jafar Sharif[6], Daisuke Takahashi[7], Koji Atarashi[8,9], Manabu Nakayama[10], Satoshi Onawa[7], Yumiko Fujimura[1,3], Masumi Takahashi[7], Tomokatsu Ikawa[9,11], Takeshi Otsubo[12], Yuki I Kawamura[12], Taeko Dohi[12], Shoji Tajima[13], Hiroshi Masumoto[14], Osamu Ohara[5], Kenya Honda[8,15], Shohei Hori[16], Hiroshi Ohno[2,4,7], Haruhiko Koseki[6] & Koji Hase[1,3,4,9,17]

Intestinal regulatory T cells (T_{reg} cells) are necessary for the suppression of excessive immune responses to commensal bacteria. However, the molecular machinery that controls the homeostasis of intestinal T_{reg} cells has remained largely unknown. Here we report that colonization of germ-free mice with gut microbiota upregulated expression of the DNA-methylation adaptor Uhrf1 in T_{reg} cells. Mice with T cell–specific deficiency in Uhrf1 (*Uhrf1*$^{fl/fl}$*Cd4*-Cre mice) showed defective proliferation and functional maturation of colonic T_{reg} cells. Uhrf1 deficiency resulted in derepression of the gene (*Cdkn1a*) that encodes the cyclin-dependent kinase inhibitor p21 due to hypomethylation of its promoter region, which resulted in cell-cycle arrest of T_{reg} cells. As a consequence, *Uhrf1*$^{fl/fl}$*Cd4*-Cre mice spontaneously developed severe colitis. Thus, Uhrf1-dependent epigenetic silencing of *Cdkn1a* was required for the maintenance of gut immunological homeostasis. This mechanism enforces symbiotic host-microbe interactions without an inflammatory response.

The mammalian fetus is maintained under sterile conditions in the uterus. However, immediately after birth, it is exposed to a multitude of environmental microbes, some of which colonize the skin and mucosal surfaces. In particular, the lumen of the human distal intestine harbors trillions of microorganisms. Notably, despite such a tremendous microbial burden in close proximity to the intestinal epithelial cells, the colonizing microbiota seldom causes inflammatory diseases. This is mainly due to the establishment of an immunoregulatory system characterized by the accumulation of mucosal Foxp3$^+$ regulatory T cells (T_{reg} cells)[1–4], which serve a pivotal role in the containment of potentially pathogenic inflammatory responses[1,5,6]. T_{reg} cells arise both in the thymus and in the periphery as a consequence of exposure to microbial antigens (for example, antigens from clusters IV and XIVa of the bacterial class Clostridia, altered Schaedler flora and *Bacteroides fragilis*)[1–4,7–10]. Although much has been learned about the development, migration[11] and function of intestinal T_{reg} cells, the molecular mechanisms by which these cells establish symbiotic host-microbe relationships without inflammation still remains to be elucidated.

Epigenetic regulation serves important roles in controlling gene expression in a heritable manner[12]. Compelling evidence has revealed active contribution of epigenetic regulation to cell-fate 'decisions' as well as to the stabilization of cell lineages during the development of various cells of the immune system, including T_{reg} cells[13–15]. Butyrate derived from Clostridia bacteria upregulates acetylation of histone H3 at the promoter and conserved-noncoding-sequence regions of the locus encoding the transcription factor Foxp3 and eventually facilitates *Foxp3* expression in naive T cells[7]. That finding supports the idea that the epigenetic status of T_{reg} cells and potentially other T cell subsets may be influenced by environmental factors, such as the cytokine milieu and microbial factors. The spatiotemporal control of the epigenetic status of T_{reg} cells should be clarified for full understanding of local development of these cells and their homeostasis in the intestine.

[1]Division of Mucosal Barriology, International Research and Development Center for Mucosal Vaccines, The Institute of Medical Science, The University of Tokyo, Tokyo, Japan. [2]Laboratory for Immune Regulation, Graduate School of Medicine, Chiba University, Chiba, Japan. [3]Laboratory for Bioenvironmental Epigenetics, RIKEN Center for Integrative Medical Sciences, Kanagawa, Japan. [4]Graduate School of Medical Life Science, Yokohama City University, Kanagawa, Japan. [5]Laboratory for Integrative Genomics, RIKEN Center for Integrative Medical Sciences, Kanagawa, Japan. [6]Laboratory for Developmental Genetics, RIKEN Center for Integrative Medical Sciences, Kanagawa, Japan. [7]Laboratory for Intestinal Ecosystem, RIKEN Center for Integrative Medical Sciences, Kanagawa, Japan. [8]Laboratory for Gut Homeostasis, RIKEN Center for Integrative Medical Sciences, Kanagawa, Japan. [9]PRESTO, Japan Science and Technology Agency, Saitama, Japan. [10]Laboratory of Medical Genomics, Department of Human Genome Research, Kazusa DNA Research Institute, Chiba, Japan. [11]Laboratory for Immune Regeneration, RIKEN Center for Integrative Medical Sciences, Kanagawa, Japan. [12]Department of Gastroenterology, Research Center for Hepatitis and Immunology, Research Institute, National Center for Global Health and Medicine, Chiba, Japan. [13]Laboratory of Epigenetics, Institute for Protein Research, Osaka University, Osaka, Japan. [14]Laboratory of Cell Engineering, Department of Frontier Research, Kazusa DNA Research Institute, Chiba, Japan. [15]CREST, Japan Science and Technology Agency, Saitama, Japan. [16]Laboratory for Immune Homeostasis, RIKEN Center for Integrative Medical Sciences, Kanagawa, Japan. [17]Present address: Department of Biochemistry, Keio University Graduate School of Pharmaceutical Science, Tokyo, Japan. [18]These authors contributed equally to this work. Correspondence should be addressed to K. Ha. (hase-kj@pha.keio.ac.jp).

Received 16 December 2013; accepted 1 April 2014; published online 28 April 2014; doi:10.1038/ni.2886

Uhrf1 ('ubiquitin-like, with pleckstrin-homology and RING-finger domains 1'; also known as Np95 in mice and ICBP90 in humans) is an epigenetic regulator that forms gene-repression complexes through its interaction with the DNA methyltransferase Dnmt1 and the histone deacetylase HDAC1 (refs. 16–19). Uhrf1 'preferentially' binds hemimethylated DNA via the SET- and RING finger–associated domain and contributes substantially to the accurate maintenance of DNA methylation by recruiting Dnmt1 to the hemimethylation sites. Therefore, ablation of Uhrf1 results in the hypomethylation of retrotransposons and 'imprinted' genes in embryonic stem cells[17].

Here we sought to elucidate the molecular entity responsible for the population expansion of T_{reg} cells on the basis of host-microbe interactions and found upregulation of Uhrf1 expression in colonic T_{reg} cells in response to bacterial colonization. The upregulation of Uhrf1 expression was essential for vigorous proliferation of colonic T_{reg} cells in response to bacterial colonization through its epigenetic silencing of the gene that encodes the cyclin-dependent kinase inhibitor p21 (*Cdkn1a*). Accordingly, mice with T cell–specific deletion of Uhrf1 spontaneously developed colitis due to defects in the proliferation and suppressive function of T_{reg} cells. We therefore reason that Uhrf1-dependent regulation of the proliferation of T_{reg} cells via this epigenetic mechanism is essential for containment of the inflammatory response to gut microbiota.

RESULT

Gut bacteria induce proliferation of colonic T_{reg} cells

To gain mechanistic insight into the maintenance of gut immunological homeostasis during the establishment of symbiotic host-microbe interactions, we orally inoculated germ-free (GF) mice of the IQI strain with commensal microbiota and monitored changes in interleukin 2 (IL-2)-expressing $CD4^+$ T cells and $Foxp3^+$ T_{reg} cell populations in the colonic lamina propria (cLP) of these formerly germ-free ('ex–germ-free' (exGF)) mice. The frequency of $IL\text{-}2^+CD4^+$ T cells peaked within 3 d of bacterial colonization and then gradually decreased to the basal frequency by day 7 (**Fig. 1a**). The kinetics of the T_{reg} cell population expansion paralleled that of the $IL\text{-}2^+CD4^+$ T cells up until day 3, but then the T_{reg} cell populations continued to expand (**Fig. 1a**) and became the dominant $CD4^+$ T cell population in the colon. The rapid population expansion of T_{reg} cells after bacterial colonization raised the possibility that the commensals may induce not just the differentiation[7,9] and migration[8] but also the local proliferation of T_{reg} cells in the cLP. Indeed, there was considerable population expansion of $Ki67^+$ proliferative T_{reg} cells after bacterial colonization (**Fig. 1a**). Proliferating (EdU^+) T_{reg} cells were much more abundant in the cLP of exGF mice than in that of GF mice (**Fig. 1b**). Differences in the expression of neuropilin-1 (Nrp1) has been proposed as a marker for distinguishing natural T_{reg} cell subsets from peripherally induced T_{reg} cell subsets[20,21]. We observed that both the $Nrp1^-Foxp3^+$ subset (T_{reg} cells that arose in the periphery) and $Nrp1^+Foxp3^+$ subset (T_{reg} cells that arose in the thymus) displayed the proliferative response, although it was more prominent in the $Nrp1^-$ population (**Fig. 1c**). This proliferative response was confined to colonic T_{reg} cells and was minimal in $CD4^+Foxp3^-$ conventional T cells (T_{conv} cells) and splenic $CD4^+Foxp3^+$ T cells (**Fig. 1b** and **Supplementary Fig. 1a**). Similarly, we observed the rapid T_{reg} cell population expansion in the cLP but not the spleen of specific pathogen–free (SPF) mice before weaning, a time during which the intestinal microflora is established (**Supplementary Fig. 1b,d**). To gain further evidence showing that the proliferation of T_{reg} cells was occurring locally in the colon, we blocked the influx of extraintestinal

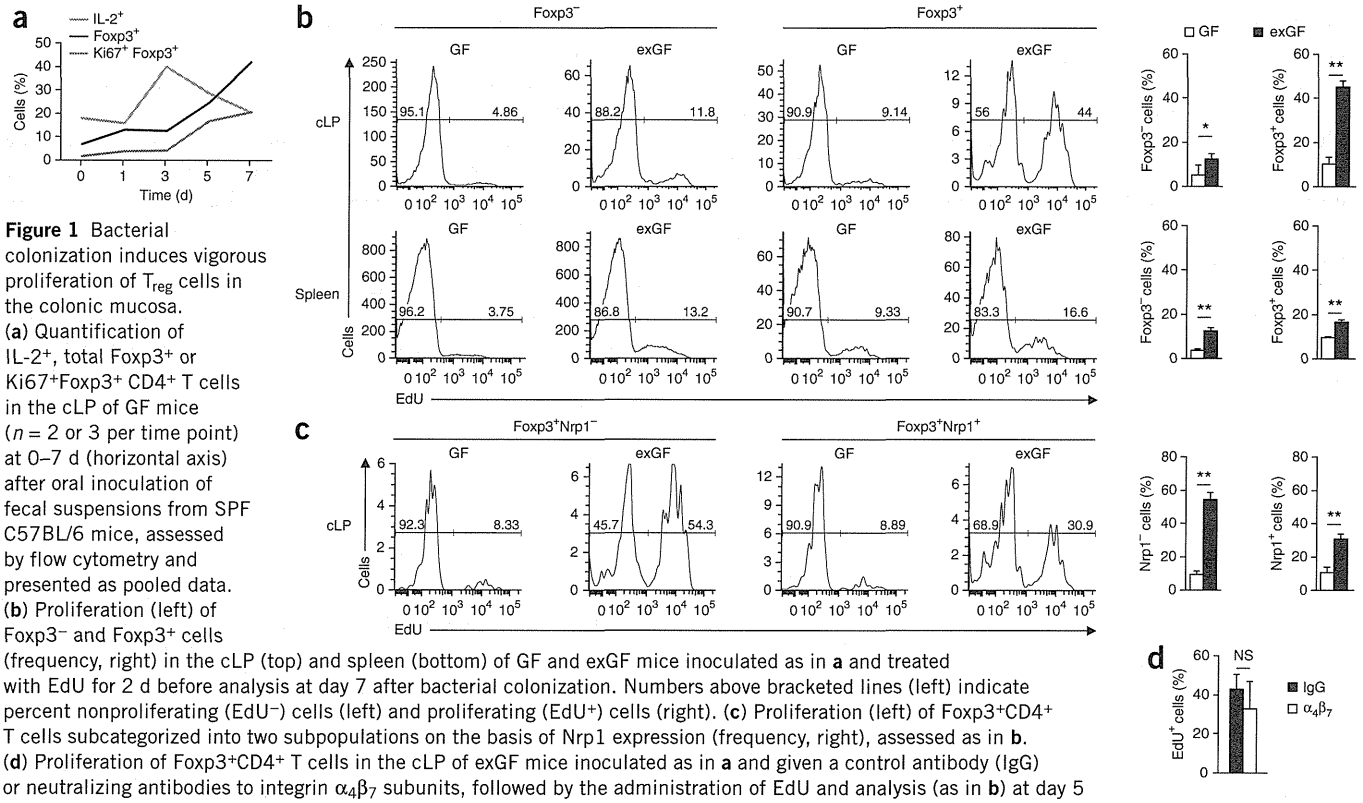

Figure 1 Bacterial colonization induces vigorous proliferation of T_{reg} cells in the colonic mucosa. (**a**) Quantification of $IL\text{-}2^+$, total $Foxp3^+$ or $Ki67^+Foxp3^+$ $CD4^+$ T cells in the cLP of GF mice ($n = 2$ or 3 per time point) at 0–7 d (horizontal axis) after oral inoculation of fecal suspensions from SPF C57BL/6 mice, assessed by flow cytometry and presented as pooled data. (**b**) Proliferation (left) of $Foxp3^-$ and $Foxp3^+$ cells (frequency, right) in the cLP (top) and spleen (bottom) of GF and exGF mice inoculated as in **a** and treated with EdU for 2 d before analysis at day 7 after bacterial colonization. Numbers above bracketed lines (left) indicate percent nonproliferating (EdU^-) cells (left) and proliferating (EdU^+) cells (right). (**c**) Proliferation (left) of $Foxp3^+CD4^+$ T cells subcategorized into two subpopulations on the basis of Nrp1 expression (frequency, right), assessed as in **b**. (**d**) Proliferation of $Foxp3^+CD4^+$ T cells in the cLP of exGF mice inoculated as in **a** and given a control antibody (IgG) or neutralizing antibodies to integrin $\alpha_4\beta_7$ subunits, followed by the administration of EdU and analysis (as in **b**) at day 5 after bacterial colonization. NS, not significant; $^*P < 0.05$ and $^{**}P < 0.01$ (Student's *t*-test). Data are representative of at least two or three independent experiments (error bars, s.d. of five (**b**,**c**) or three (**d**) mice).

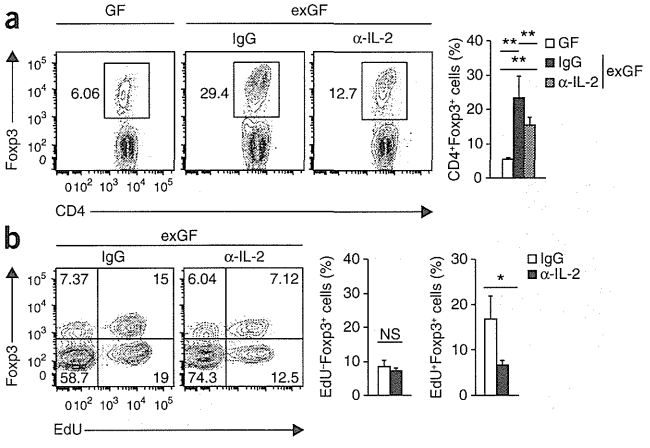

Figure 2 IL-2 is responsible for the vigorous proliferation of colonic T_{reg} cells after inoculation of commensal bacteria. (**a**) Foxp3 expression by CD4+ T cells in the cLP of GF mice left untreated and exGF mice inoculated with bacteria (as in **Fig. 1a**) and, 3 d later, given intravenous injection of control IgG or IL-2-neutralizing antibody (α-IL-2) and assessed 2 d later. Numbers adjacent to outlined areas (left) indicate percent Foxp3+CD4+ T cells. (**b**) Proliferation of CD4+ T cells in the cLP of exGF mice treated as in **a**. Numbers in quadrants (left) indicate percent cells in each. $*P < 0.05$ and $**P < 0.01$ (one-way analysis of variance (ANOVA) followed by Tukey's test (**a**) or Student's *t*-test (**b**)). Data are representative of at least three independent experiments (error bars, s.d. of three mice).

T_{reg} cells with neutralizing antibodies to integrin $\alpha_4\beta_7$ subunits[11] before administering the thymidine analog EdU to exGF mice. This treatment affected the abundance of proliferative T_{reg} cells in the colon only marginally (**Fig. 1d**). Collectively, these results suggested that colonization by commensal bacteria induced extensive proliferation of T_{reg} cells mainly in the colonic mucosa.

IL-2 is responsible for colonic T_{reg} cell population expansion

IL-2, which is well documented as promoting the proliferation of T_{reg} cells[22], was induced in the colonic mucosa, particularly in CD4+ T cells after inoculation of mice with bacteria (**Fig. 1a**). Similarly, colonic CD4+ T cells of infant mice (around 2 weeks old) housed in SPF conditions had high expression of IL-2; during this time, T_{reg} cells displayed active proliferation in the cLP but not in the spleen (**Supplementary Fig. 1b,d**). We therefore postulated that early induction of IL-2 may have been responsible for the local proliferation of T_{reg} cells. To test this idea, we treated exGF mice with neutralizing antibody to IL-2. As expected, abrogation of IL-2 strongly suppressed the induction of colonic T_{reg} cells (**Fig. 2a**). There was also a significantly lower abundance of EdU+ proliferating T_{reg} cells in the antibody-treated exGF mice than in their counterparts treated with the control antibody immunoglobulin G (IgG) (**Fig. 2b**). On the basis of these observations, we reasoned that an early IL-2 response was indispensable for the proliferation of T_{reg} cells in the colon.

IL-2 upregulates *Uhrf1* in colonic T_{reg} cells

We explored the molecular machinery that mediates the proliferation of colonic T_{reg} cells. First we profiled genes selectively upregulated in T_{reg} cells from exGF mice (**Fig. 3a**, cluster I). We also categorized IL-2-responsive genes (**Fig. 3b**, cluster II). After comparison of the two clusters, followed by gene ontology–based functional analysis, we selected several candidate genes encoding molecules potentially associated with the proliferation of colonic T_{reg} cells in an IL-2-dependent manner (**Fig. 3c**). Among those specifically upregulated in colonic T_{reg} cells was *Uhrf1* (**Fig. 3d**). *Uhrf1* expression was highest in T_{reg} cells among colonic CD4+ T cell subsets in SPF mice (**Fig. 3e**). We confirmed that IL-2 was essential for *Uhrf1* expression by colonic T_{reg} cells after inoculation of commensals, since neutralization of IL-2 in exGF mice significantly inhibited *Uhrf1* expression (**Fig. 3f**). In contrast, *Uhrf1* was not induced in splenic T_{reg} cells from exGF mice (**Supplementary Fig. 1e**). Consistent with our observations of exGF mice, there was substantial upregulation of *Uhrf1* in colonic T_{reg} cells during the population-expansion phase in infant SPF mice (**Supplementary Fig. 1c**).

To rigorously confirm the role of bacterial colonization in *Uhrf1* expression, we analyzed gnotobiotic mice colonized with a 17-strain mixture of Clostridia bacteria ('17-mix'), which efficiently induces the population expansion of T_{reg} cells in the colon[23]. Inoculation of GF mice with 17-mix significantly augmented IL-2 expression by T_{conv} cells (**Fig. 3g**), which led to upregulation of *Uhrf1* in T_{reg} cells, with a concomitant increase in their proliferation (**Fig. 3h,i**). We also confirmed the upregulation of *Uhrf1* in cultured T_{reg} cells stimulated with IL-2 (**Fig. 3j**), in which accumulation of the transcription factor STAT5 on the promoter region of *Uhrf1* was also evident (**Fig. 3k**). Together these results indicated that commensal bacteria upregulated *Uhrf1* in T_{reg} cells by eliciting IL-2 production from effector T cells (T_{eff} cells) in the colonic mucosa.

Uhrf1 is critical for colonic T_{reg} cell proliferation

To investigate the role of Uhrf1 in the homeostasis of colonic T_{reg} cells, we generated mice with T cell–specific deficiency in Uhrf1 (mice with *lox*P-flanked alleles (*Uhrf1*$^{fl/fl}$) deleted by Cre recombinase expressed from the Cd4 promoter (*Uhrf1*$^{fl/fl}$*Cd4*-Cre mice); **Supplementary Fig. 2a**) and crossed them with *Foxp3*^{hCD2} reporter mice (which have sequence encoding a reporter fusion of human CD52 and CD2 inserted into *Foxp3*), to easily detect T_{reg} cells[14], and thus generated *Uhrf1*$^{fl/fl}$*Cd4*-Cre*Foxp3*^{hCD2} progeny (called '*Uhrf1*$^{fl/fl}$*Cd4*-Cre' here). In young *Uhrf1*$^{fl/fl}$*Cd4*-Cre mice reared under SPF conditions, the overall composition of B lymphocytes and T lymphocytes was intact (**Supplementary Fig. 2b,c**). However, these mice had a considerable defect in the development of colonic T_{reg} cells (**Fig. 4a**) indicative of the importance of Uhrf1 in the homeostasis of T_{reg} cells in the colonic mucosa. We observed a slightly lower abundance of T_{reg} cells in the spleen and thymus of *Uhrf1*$^{fl/fl}$*Cd4*-Cre mice than in those of their *Uhrf1*$^{+/+}$*Cd4*-Cre (control) littermates (**Supplementary Fig. 2d**). We also confirmed the lower abundace of colonic T_{reg} cells in chimeras reconstituted with a mixture of bone marrow progenitor cells from Uhrf1-deficient and congenic wild-type mice. T_{reg} cells derived from the bone marrow of Uhrf1-deficient mice were nearly completely absent from the chimeras (**Supplementary Fig. 3a–c**). Thus, a T_{reg} cell–intrinsic defect was the cause of the lower abundance of these cells. Collectively, these data demonstrated that Uhrf1 was essential for the maintenance of colonic T_{reg} cells but not for the maintenance of extracolonic T_{reg} cells.

We further investigated whether Uhrf1 deficiency affected the differentiation or proliferation of T_{reg} cells by both *in vitro* and *in vivo* experiments. Uhrf1 deficiency did not influence the differentiation or stability of Foxp3 expression by T_{reg} cells in an *in vitro* culture system (**Fig. 4b** and data not shown). To rigorously confirm those results, we transferred naive CD4+ T cells from Uhrf1-deficient or Uhrf1-sufficient CD45.2+ mice into CD45.1+ mice. The efficiency of T_{reg} cell differentiation *in vivo* was similar for Uhrf1-deficient and Uhrf1-sufficient naive T cells (**Supplementary Fig. 4a,b**). In contrast,

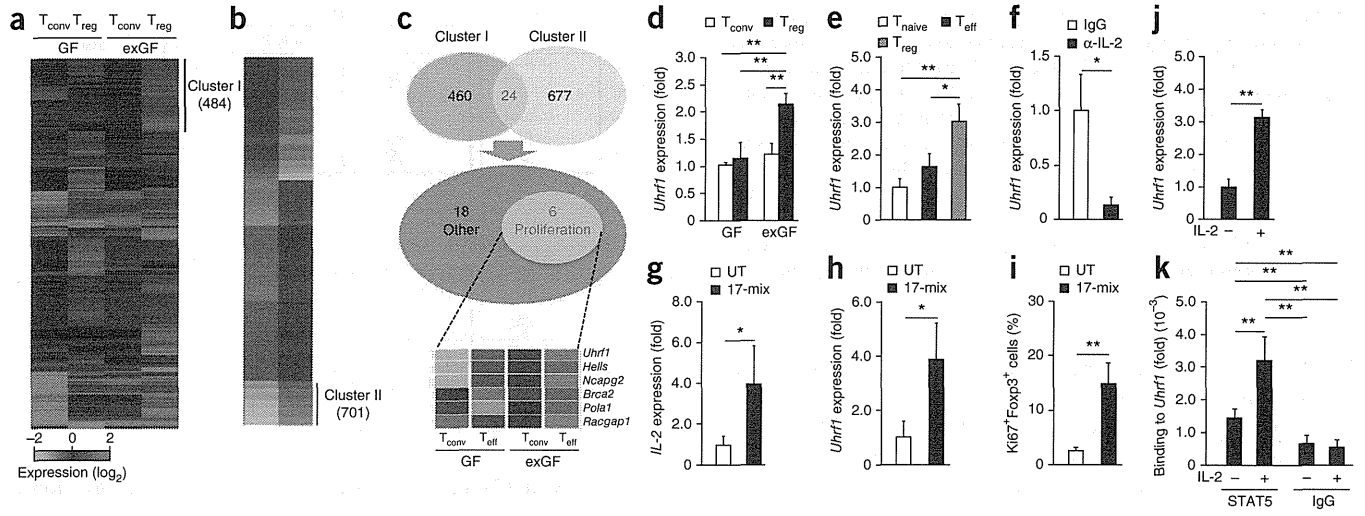

Figure 3 Colonization with commensal bacteria induces *Uhrf1* expression in colonic T_{reg} cells in IL-2-dependent manner. (**a**) Gene-expression profiles of T_{conv} cells ($CD3\varepsilon^+CD4^+CD25^-FR4^-$) and T_{reg} cells ($CD3\varepsilon^+CD4^+CD25^+FR4^+$) isolated from the cLP of GF and exGF mice. (**b**) Gene-expression profile of T_{reg} cells obtained from SPF mice and cultured *in vitro* and stimulated for 2 d with IL-2 in the presence of TGF-β. (**c**) Gene ontology–enrichment analysis of genes common to clusters I and II in **a**,**b**. (**d**) Quantitative PCR analysis of *Uhrf1* expression in T_{conv} cells and T_{reg} cells from the cLP of GF and exGF mice at 7 d after oral inoculation with feces from SPF C57BL/6 mice; results were normalized to those of the gene encoding β-actin (*Actb*) and are presented relative to those of T_{conv} cells from GF mice, set as 1. (**e**) *Uhrf1* expression in naive T cells (T_{naive}; $CD3\varepsilon^+CD4^+hCD2^-CD44^{lo}CD62L^{hi}$), T_{eff} cells ($CD3\varepsilon^+CD4^+hCD2^-CD44^{hi}CD62L^{lo}$) and T_{reg} cells $CD3\varepsilon^+CD4^+hCD2^+$) from SPF *Foxp3*^{hCD2} mice; results were normalized as in **d** and are presented relative to those of naive T cells, set as 1. (**f**) Quantitative PCR analysis of *Uhrf1* expression in cells from the cLP of mice inoculated orally with feces from SPF C57BL/6 mice and then, 3 d later, given intravenous injection of control IgG or neutralizing antibody to IL-2, followed by analysis 2 d later (at day 5); results were normalized as in **d** and are presented relative to those of cells from mice treated with IgG, set as 1. (**g**,**h**) Quantitative PCR analysis of the expression of *Il2* in T_{conv} cells (**g**) and *Uhrf1* in T_{reg} cells (**h**) from GF mice at day 3 (**g**) or day 6 (**h**) after inoculation with 17-mix; results were normalized to those of the gene encoding ribosomal protein L13A (*Rpl13a*) are presented relative to those of cells from untreated GF mice (UT), set as 1. (**i**) Frequency of $Foxp3^+Ki67^+$ cells in the cLP of GF mice at day 6 after inoculation with 17-mix, analyzed by flow cytometry (presented as in **g**,**h**). (**j**) Quantitative PCR analysis of *Uhrf1* expression in splenic $CD4^+CD25^+$ T cells cultured for 3 d with beads coated with mAb to CD3 and mAb to CD28 in the presence of IL-2 and TGF-β, allowed to 'rest' for 6 h and then stimulated 24 h with (+) or without (–) IL-2; results were normalized as in **g**,**h** and are presented relative to those of cells not stimulated with IL-2, set as 1. (**k**) ChIP–quantitative PCR analysis of the binding of STAT5 or IgG to the *Uhrf1* promoter region in splenic T cells cultured with beads as in **j**, allowed to 'rest' for 6 h and then stimulated for 1.5 h with or without IL-2; results are presented relative to total input. $^*P < 0.05$ and $^{**}P < 0.01$ (one-way ANOVA followed by Tukey's test (**d**,**e**,**k**), Mann-Whitney *U*-test (**f**,**g**,**i**) or Student's *t*-test (**h**,**j**)). Data are representative of one experiment (**a**–**c**,**g**–**k**;) or two experiments (**d**–**f**; error bars, s.e.m (**d**) or s.d. (**e**–**k**) of three mice per group).

Uhrf1 deficiency substantially adversely affected proliferation due to cell-cycle arrest at the G1-S transition (**Fig. 4c**,**d**). The same was true for Uhrf1-deficient T_{reg} cells in the cLP, as the frequency of $Ki67^+$ proliferating $Foxp3^+$ T_{reg} cells in the colon of *Uhrf1*$^{fl/fl}$*Cd4*-Cre mice was diminished (**Fig. 4e**,**f**). In contrast, the proliferation of T_{conv} cells was unaffected by Uhrf1 deficiency (**Fig. 4e**).

We further confirmed the role of Uhrf1 in T_{reg} cell homeostasis by another *in vivo* experiment. Although there was no difference between *Uhrf1*$^{fl/fl}$*Cd4*-Cre and *Uhrf1*$^{+/+}$*Cd4*-Cre mice in their proportion of T_{reg} cells under GF conditions (**Fig. 4g**), *Uhrf1*$^{fl/fl}$*Cd4*-Cre mice had defective population expansion of T_{reg} cells in response to colonization by chloroform-resistant bacteria, which consist of spore-forming bacteria mainly of the class Clostridia[1,24] (**Fig. 4h**). Thus, Uhrf1 was indispensable for the local population expansion of colonic T_{reg} cells.

Given that *Uhrf1* was an IL-2-responsive gene, we postulated the IL-2–Uhrf1 axis may serve a key role in the extensive proliferation of T_{reg} cells. To further investigate this possibility, we treated *Uhrf1*$^{fl/fl}$ *Cd4*-Cre and *Uhrf1*$^{+/+}$*Cd4*-Cre mice with exogenous IL-2 mixed with monoclonal antibody (mAb) to IL-2 (i.e., as a complex of IL-2 and mAb to IL-2). Consistent with a published report[25], this treatment potently induced a proliferative response in the systemic T_{reg} cell population specifically in *Uhrf1*$^{+/+}$*Cd4*-Cre mice; however, this response was substantially attenuated in the same population from *Uhrf1*$^{fl/fl}$*Cd4*-Cre mice (**Fig. 4i**). The complex of IL-2 and mAb to IL-2 also induced the proliferation of T_{conv} cells, albeit to a lesser extent than that of T_{reg} cells regardless of the presence of Uhrf1. These data provided evidence of the notable role of the IL-2–Uhrf1 axis in T_{reg} cell proliferation but the lesser role of this axis for T_{conv} cells.

Proliferation may confer functional maturity to T_{reg} cells[26], as shown by upregulation of the expression of molecules with a suppressive function in the proliferative compartment (**Supplementary Fig. 5a**). We hypothesized that diminished proliferative activity in the absence of Uhrf1 may affect the suppressive activity of T_{reg} cells. Indeed, ablation of Uhrf1 impaired the expression of functional molecules, including IL-10 and the immunomodulatory receptor CTLA-4 (CD152) (**Fig. 4j** and **Supplementary Fig. 5b**). Accordingly, Uhrf1-deficient T_{reg} cells exhibited attenuated immunosuppressive function and failed to prevent the development of experimental colitis (**Supplementary Fig. 6**). Given these observations, we concluded that Uhrf1 serves an essential role in the functional maturation of T_{reg} cells in the colonic mucosa, probably by regulating proliferation.

Uhrf1 epigenetically represses *Cdkn1a* expression

The Uhrf1-Dnmt1 complex has a critical role in the accurate maintenance of DNA methylation, which contributes to gene repression[16,17]. To define the targets of Uhrf1 that encode molecules involved in T_{reg} cell proliferation, we first profiled the subset of genes specifically derepressed only in T_{reg} cells (**Supplementary Fig. 7a**). Gene-function–enrichment analysis of the genes profiled identified at the top of the

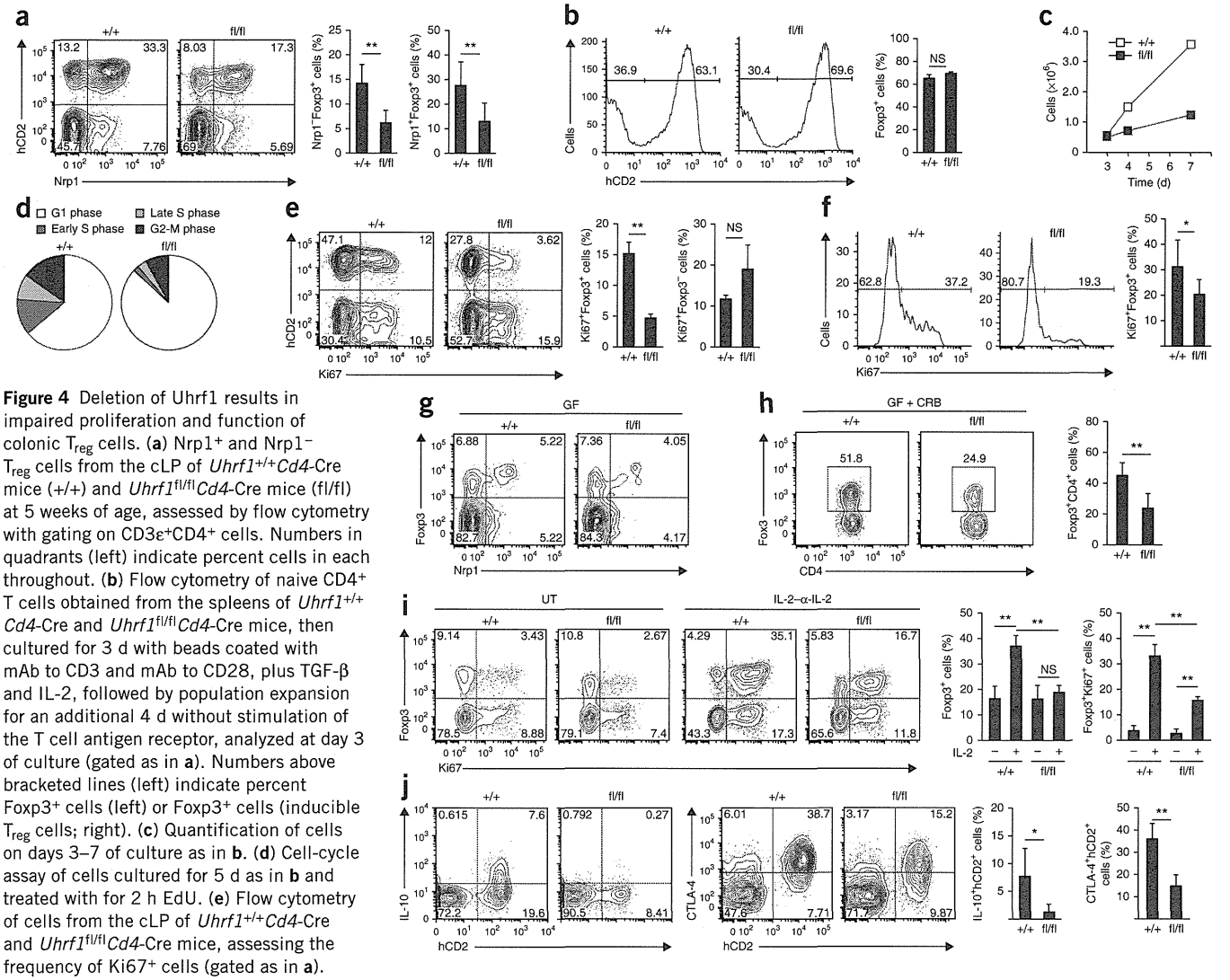

Figure 4 Deletion of Uhrf1 results in impaired proliferation and function of colonic T_{reg} cells. (**a**) Nrp1$^+$ and Nrp1$^-$ T_{reg} cells from the cLP of *Uhrf1*$^{+/+}$*Cd4*-Cre mice (+/+) and *Uhrf1*$^{fl/fl}$*Cd4*-Cre mice (fl/fl) at 5 weeks of age, assessed by flow cytometry with gating on CD3ε$^+$CD4$^+$ cells. Numbers in quadrants (left) indicate percent cells in each throughout. (**b**) Flow cytometry of naive CD4$^+$ T cells obtained from the spleens of *Uhrf1*$^{+/+}$ *Cd4*-Cre and *Uhrf1*$^{fl/fl}$*Cd4*-Cre mice, then cultured for 3 d with beads coated with mAb to CD3 and mAb to CD28, plus TGF-β and IL-2, followed by population expansion for an additional 4 d without stimulation of the T cell antigen receptor, analyzed at day 3 of culture (gated as in **a**). Numbers above bracketed lines (left) indicate percent Foxp3$^+$ cells (left) or Foxp3$^+$ cells (inducible T_{reg} cells; right). (**c**) Quantification of cells on days 3–7 of culture as in **b**. (**d**) Cell-cycle assay of cells cultured for 5 d as in **b** and treated with for 2 h EdU. (**e**) Flow cytometry of cells from the cLP of *Uhrf1*$^{+/+}$*Cd4*-Cre and *Uhrf1*$^{fl/fl}$*Cd4*-Cre mice, assessing the frequency of Ki67$^+$ cells (gated as in **a**). (**f**) Flow cytometry of cells as in **e**, but with gating on CD3ε$^+$CD4$^+$Foxp3$^+$ cells. (**g**) Expression of Foxp3 and Nrp1 by CD4$^+$ T cells from the cLP of 8-week-old *Uhrf1*$^{+/+}$*Cd4*-Cre and *Uhrf1*$^{fl/fl}$*Cd4*-Cre mice reared under GF conditions, analyzed by flow cytometry (gated as in **a**). (**h**) Flow cytometry of CD4$^+$ T cells from the cLP of mice as in **g**, inoculated with chloroform-resistant bacteria (+ CRB) and analyzed 4 weeks later (gated as in **a**). Numbers adjacent to outline areas indicate percent Foxp3$^+$CD4$^+$ T cells. (**i**) Expression of Foxp3 and Ki67 by splenic CD4$^+$ T cells from *Uhrf1*$^{+/+}$*Cd4*-Cre and *Uhrf1*$^{fl/fl}$*Cd4*-Cre mice left untreated (UT) or treated with complexes of IL-2 and mAb to IL-2 (IL-2–α-IL-2), analyzed by flow cytometry (gated as in **a**). (**j**) Expression of IL-10 and CTLA-4 by Foxp3$^+$ cells from the cLP of *Uhrf1*$^{+/+}$*Cd4*-Cre and *Uhrf1*$^{fl/fl}$*Cd4*-Cre mice raised under SPF conditions, analyzed by flow cytometry (gated as in **a**). $^*P < 0.05$ and $^{**}P < 0.01$ (Student's *t* test (**a**,**e**,**f**,**h**,**j**), Mann-Whitney *U*-test (**b**) or one-way ANOVA followed by Tukey's test (**i**)). Data are representative of three independent experiments (error bars, s.d. of four to nine mice per group).

list (that is, among genes with the highest statistical significance) a group of genes encoding molecules in the category of 'cellular growth and proliferation' (**Supplementary Fig. 7b**,**c**). Furthermore, we used an integrated '-omics' approach with data sets obtained from the transcriptome and analysis of the 'methylome' (the pattern of methylated DNA in the genome) based on precipitation of methylated DNA followed by sequencing (MeDP-seq) (**Fig. 5a**) and identified *Cdkn1a* as a target of Uhrf1 (**Fig. 5b**). The product of *Cdkn1a*, p21, is a cell-cycle regulator that induces cell-cycle arrest at the G1-S transition[27]. We confirmed that there was substantially more *Cdkn1a* mRNA and p21 protein in *Uhrf1*$^{fl/fl}$*Cd4*-Cre T_{reg} cells than in *Uhrf1*$^{+/+}$*Cd4*-Cre T_{reg} cells (**Fig. 5c**,**d**). The derepression of *Cdkn1a* most probably resulted from hypomethylation of CpG islands in the distal promoter region of *Cdkn1a* in the absence of Uhrf1 (**Fig. 5e–g**), an outcome that was more prominent in T_{reg} cells than in T_{conv} cells (**Fig. 5f**). To further explore whether the derepression of *Cdkn1a* caused the cell-cycle arrest of *Uhrf1*$^{fl/fl}$*Cd4*-Cre T_{reg} cells, we induced *Uhrf1*$^{fl/fl}$*Cd4*-Cre cells *in vitro* to differentiate into T_{reg} cells, then treated those cells with small interfering RNA (siRNA) targeting *Cdkn1a* and analyzed their cell-cycle status. Knockdown of *Cdkn1a*, which diminished *Cdkn1a* expression by 45% (data not shown), at least partially rescued cells from the arrest at G1, as indicated by the greater proportion of cells in S phase than in G2-M phases (**Fig. 5h**). From these data, we concluded that Uhrf1-dependent repression of *Cdkn1a* was critical for the maintenance of T_{reg} cell proliferation.

Uhrf1-deficient mice spontaneously develop colitis

Intestinal T_{reg} cells orchestrate the immunoregulatory system that suppresses inappropriate immune responses to commensal bacteria[28].